A young testicular microenvironment protects Leydig cells against agerelated dysfunction in a mouse model of premature aging

THE FASEB JOURNAL • RESEARCH • www.fasebj.org

A young testicular microenvironment protects Leydig cells against age-related dysfunction in a mouse model of premature aging

Michael Curley,* Laura Milne,* Sarah Smith,* Anne Jørgensen,†,‡ Hanne Frederiksen,†,‡ Patrick Hadoke,§ Paul Potter,¶ and Lee B. Smith*,‖,1

*Medical Research Council (MRC) Centre for Reproductive Health and §The British Heart Foundation Centre for Cardiovascular Science, University of Edinburgh, The Queen's Medical Research Institute, Edinburgh, United Kingdom; †Department of Growth and Reproduction, and ‡International Centre for Research and Research Training in Endocrine Disruption of Male Reproduction and Child Health, Rigshospitalet, University of Copenhagen, Copenhagen, Denmark; ¶MRC Mammalian Genetics Unit, MRC Harwell, Harwell, United Kingdom; and ‖School of Environmental and Life Sciences, University of Newcastle, Callaghan, New South Wales, Australia

ABSTRACT: Testicular Leydig cells (LCs) are the primary source of circulating androgen in men. As men age, circulating androgen levels decline. However, whether reduced LC steroidogenesis results from specific effects of aging within LCs or reflects degenerative alterations to the wider supporting microenvironment is unclear; inability to separate intrinsic LC aging from that of the testicular microenvironment *in vivo* has made this question difficult to address. To resolve this, we generated novel mouse models of premature aging, driven by CDGSH iron sulfur domain 2 (*Cisd2*) deletion, to separate the effects of cell intrinsic aging from extrinsic effects of aging on LC function. At 6 mo of age, constitutive *Cisd2*-deficient mice display signs of premature aging, including testicular atrophy, reduced LC and Sertoli cell (SC) number, decreased circulating testosterone, increased luteinizing hormone/testosterone ratio, and decreased expression of steroidogenic mRNAs, appropriately modeling primary testicular dysfunction observed in aging men. However, mice with *Cisd2* deletion (and thus premature aging) restricted to either LCs or SCs were protected against testicular degeneration, demonstrating that age-related LCs dysfunction cannot be explained by intrinsic aging within either the LC or SC lineages alone. We conclude that age-related LC dysfunction is largely driven by aging of the supporting testicular microenvironment.—Curley, M., Milne, L., Smith, S., Jørgensen, A., Frederiksen, H., Hadoke, P., Potter, P., Smith, L. B. A Young testicular microenvironment protects Leydig cells against age-related dysfunction in a mouse model of premature aging. FASEB J. 33, 000–000 (2019). www.fasebj.org

KEY WORDS: testis · testosterone · gonadotropin · steroidogenesis

The mammalian testis is divided into 2 distinct compartments that perform its principal functions. Spermatogenesis occurs within the seminiferous tubules, and androgen biosynthesis occurs in the interstitial space. Both of these processes are entirely dependent on the 2 major testicular somatic cell populations—the Sertoli cells (SCs) and Leydig cells (LCs), respectively. In human males, testicular function declines during the aging process [reviewed in Perheentupa and Huhtaniemi (1) and Gunes *et al.* (2)]. Of particular significance is the reported age-related decrease in LC androgen production (3–7) because androgens have been suggested to have a crucial role in supporting lifelong general health in men, with low circulating testosterone linked to an increased risk of developing chronic age-related cardiometabolic diseases (8–13). Therefore, elucidating the mechanisms governing the maintenance and function LCs is pertinent to our understanding of male health.

ABBREVIATIONS: ABP, androgen binding protein; *Amh*, anti-Müllerian hormone; CISD2, CDGSH iron sulfur domain 2; *Cisd2*$^{tm1c(EUCOMM)Wtsi}$, KO-first conditional allele; COUP-TFII, chicken ovalbumin upstream promoter transcription factor II; Cre, cyclic recombinase; hCG, human chorionic gonadotropin; H&E, hematoxylin and eosin; HET, heterozygous; HPG, hypothalamic, pituitary, gonadal; HSD3B, 3β-hydroxysteroid dehydrogenase; KO, knockout; LC, Leydig cell; LH, luteinizing hormone; *Pdgfrb*, platelet-derived growth factor β; RFP, red fluorescent protein; ROS, reactive oxygen species; SC, Sertoli cell; SHBG, sex hormone binding globulin; SOX9, SRY-box 9; WT, wild type

[1] Correspondence: Medical Research Council (MRC) Centre for Reproductive Health, University of Edinburgh, The Queen's Medical Research Institute, 47 Little France Crescent, Edinburgh EH16 4TJ, United Kingdom. E-mail: lee.smith@ed.ac.uk

doi: 10.1096/fj.201800612R
This article includes supplemental data. Please visit *http://www.fasebj.org* to obtain this information.

LC androgen production is under negative feedback control from the hypothalamic-pituitary-gonad (HPG) axis. Gonadotropin-releasing hormone, from the hypothalamus, stimulates the pituitary to secrete luteinizing hormone (LH), which stimulates LC testosterone production. Increased circulating testosterone then negatively regulates the hypothalamic–pituitary unit to control LH secretion. Reduced levels of circulating testosterone (hypogonadism) can be due to defective androgen biosynthesis at the level of the LC, usually accompanied by a compensatory increase in LH and subsequent distortion of the LH/testosterone ratio (primary hypogonadism) or as a result of diminished LH production by the hypothalamic pituitary unit (secondary hypogonadism). In aging males, the former is generally observed, although testosterone levels may remain within reference range because of a compensatory increase in LH (6, 14).

Current models for the study of age-related LC dysfunction are limited. The most widely used model has been the naturally aged brown Norway rat (*Rattus norvegicus*), which has provided significant insight into changes occurring in LCs during aging, including disruption of the pro/antioxidant balance, impaired LH-receptor signal transduction and cholesterol trafficking, and reduced expression and activity of enzymes involved in the conversion of cholesterol to testosterone (15–24). Interestingly, experimentally induced regeneration of LCs through ethylene dimethane sulfonate–mediated ablation in the aged testis was, for many years, thought to reinvigorate the regenerated LC population to function as young LCs (25). More recently, it has been shown that this capacity is not maintained long term (26), suggesting that either the aging of the LC stem cells themselves is a factor or that the aged microenvironment the regenerated LCs are in is unable to support continued testosterone production. A detailed dissection of this paradigm has been hampered by both the inability to separate individual components of the system (*i.e.*, other testicular somatic cell populations that may influence LC function in a paracrine manner) and the prohibitive time and financial outlay required to study aged cohorts.

Rodent models of premature aging provide an attractive alternative for the expedited study of age-related processes. Indeed, a number of progeroid mouse lines have been generated to date, primarily through disruption of genes required for DNA repair/genomic stability or lamin processing/maintenance of nuclear architecture [reviewed in Kõks *et al.* (27) and Carrero *et al.* (28). However, most have been generated to model monogenic human progeroid syndromes and, thus, may be of limited utility for the study of age-related HPG axis dysfunction. Furthermore, in such models of constitutive gene ablation, it is difficult to separate the contribution of specific tissue/cell types to the observed phenotypes. As such, new models that provide a platform to study the mechanisms by which testis/LC function deteriorates during aging/disease are required. Ideally, a model permitting the separation of individual components of the system (*i.e.*, other somatic cell populations that may influence LC function in a paracrine manner) would be valuable in assessing cause and effect.

To that end, we first validated a novel knockout (KO)-first conditional allele [$Cisd2^{tm1a(EUCOMM)Wtsi}$] of a previously reported premature aging model driven by CDGSH iron sulfur domain 2 (CISD2) deficiency (29). CISD2 is a redox active protein localized to the endoplasmic reticulum and is thought to be important for the maintenance of endoplasmic reticulum and mitochondrial structure and function (30). In mice, *Cisd2* expression decreases with age, and its deletion results in a phenotype resembling premature aging, characterized by nerve and muscle degeneration, osteopenia, reduced body weight, and premature death (29). Conversely, *Cisd2* overexpression has been reported to delay aging in mice (31). In the present studies, we sought to characterize the testicular phenotype of constitutive and cell-specific *Cisd2*-deficient mice to assess the utility of that premature aging model for the study of age-related LC dysfunction, and determine which cell types control and/or support LC function during the aging process.

MATERIALS AND METHODS

Ethics statement

Animals were bred and maintained in strict compliance with the Animals (Scientific Procedures) Act, 1986. All procedures were conducted in accordance with United Kingdom Home Office regulations under project licenses 60/4200 and 70/8804 held by L.B.S.

Breeding of transgenic mice

Mice carrying $Cisd2^{tm1a(EUCOMM)Wtsi}$ were obtained from the International Mouse Phenotyping Consortium (IMPC; Project *http://www.mousephenotype.org/*). Male and female $Cisd2^{wt/tm1a}$ mice were intercrossed to generate $Cisd2^{wt/wt}$, $Cisd2^{wt/tm1a}$, and $Cisd2^{tm1a/tm1a}$ offspring [hereafter referred to as wild-type (WT), heterozygous (HET), and KO mice, respectively]. Mice carrying $Cisd2^{tm1c(EUCOMM)Wtsi}$ were also obtained from the IMPC Project and bred to red fluorescent protein (RFP) cyclic recombinase (Cre)-reporter mice [*B6;129S6-Gt(ROSA)26Sor*$^{tm14(CAG-tdTomato)Hze}$*/J*; referred to as tdTomato, hereafter] to generate a colony of mice carrying both transgenes ($Cisd2^{tm1c/tm1c}$;$tdTomato^{+/-}$). LC and SC–$Cisd2^{tm1c(EUCOMM)Wtsi}$ mice were generated, using *Pdgfrb*-Cre (32) mice (provided by Prof. Neil Henderson, University of Edinburgh, Edinburgh, United Kingdom) and anti-Müllerian hormone (*Amh*)-Cre (33) mice, respectively. First, $Cisd2^{tm1c/tm1c}$;$tdTomato^{+/-}$ mice were mated with either Cre line to generate $Cre^{+/-}$;$Cisd2^{wt/tm1c}$;$tdTomato^{+/-}$ and $Cre^{-/-}$;$Cisd2^{wt/tm1c}$;$tdTomato^{+/-}$ offspring. $Cre^{+/-}$;$Cisd2^{wt/tm1c}$;$tdTomato^{+/-}$ and $Cre^{-/-}$;$Cisd2^{wt/tm1c}$;$tdTomato^{+/-}$ offspring were then intercrossed to obtain $Cre^{-/-}$;$Cisd2^{tm1c/tm1c}$;$tdTomato^{+/-}$ and $Cre^{+/-}$;$Cisd2^{tm1c/tm1c}$;$tdTomato^{+/-}$ offspring (the experimental animals; hereafter referred to as LC-WT or SC-WT and LC-KO or SC-KO, respectively). Genomic DNA isolated from tail or ear biopsies was used to genotype mice for the presence of the various transgenes by standard PCR techniques using either BioMix PCR Reaction Buffer (Bioline, London, United Kingdom) or Type-it Mutation Detect PCR Kit (Qiagen, Hilden, Germany), according to the manufacturer's instructions. The details of the genotyping assays are listed in **Table 1**. For *Pdgfrb*-Cre, *Amh*-Cre, and *tdTomato* genotyping assays, primers against endogenous *Il2* were included as a positive control for the PCR reaction. Representative gels

TABLE 1. *Primers used for genotyping assays*

Assay	Primer sequence, 5′–3′	
	Forward	Reverse
Cisd2^{tm1a}		
5′-HA WT	GAATATTCAATGTGTAAAGGTTTCAA	
3′-HA WT		GAAAACATTTTCACTCCTTTCTTTTT
5′-HA MUT		GAACTTCGGAATAGGAACTTCG
Cisd2^{tm1c} Tm1c	GAGTAAGTTGACTGATCAGG	CCTATCTCATTAGATCTGCT
Cisd2^{tm1d}		
5′Cas	AAGGCGCATAACGATACCAC	
Cisd2 WT		GAAAACATTTTCACTCCTTTCTTTTT
3′ LoxP		ACTGATGGCGAGCTCAGACC
Pdgfrb-Cre	TGCCACGACCAAGTGACAGCA	AGAGACGGAAATCCATCGCTC
Amh-Cre	CACATCAGGCCCAGCTCTAT	GTGTACAGGATCGGCTCTGC
Td-tomato	CTGTTCCTGTACGGCATGG	GGCATTAAAGCAGCGTATCC
Il2	CTAGGCCACAGAATTGAAAGATCT	GTAGGTGGAAATTCTAGCATCATCC

showing PCR patterns for each assay are shown in Supplemental Fig. S1. In LC-KO and SC-KO mice, *Cisd2* recombination (*i.e.*, conversion of *Cisd2*^{tm1c} to *Cisd2*^{tm1d}) was assessed in genomic DNA isolated from testis biopsies. PCR products were analyzed with the Qiaxcel Capillary Electrophoresis System (Qiagen).

Tissue collection

Animals were euthanized between the hours of 08:00 and 11:00 AM, by methods conforming to Schedule 1 of the Animals (Scientific Procedures) Act, 1986. For adult animals [5.7 ± 0.13 mo old (means ± SEM); referred to as 6 mo old, hereafter, unless otherwise stated], this was achieved by exposure to an increasing concentration of carbon dioxide, followed by confirmation of permanent cessation of the circulation by palpitation. Where human chorionic gonadotropin (hCG) stimulation of LCs was performed, mice were injected intraperitoneally with a single dose of hCG (Chorulon; Henry Schein, Melville, NY, USA) 16 h before euthanasia (20 IU in 100 μl saline). For embryonic ages, pregnant dams were dispatched as described above, and the fetuses rapidly removed and decapitated. Body weight, testis weight, and seminal vesicle weight were recorded, and tissues were either frozen on dry ice for storage at −80°C or immersed in Bouin's fixative (Clin-Tech, Guildford, United Kingdom) for 6 h. Fixed tissues were processed, embedded in paraffin wax, and sectioned at 5 μm for histologic analysis. Tissues expressing the tdTomato-fluorescent Cre-reporter were imaged with an MZFLIII Fluorescence Stereomicroscope (Leica Biosystems, Wetzlar, Germany) fitted with a CoolSnap camera (Photometrics, Tucson, AZ, USA) and PMCapture Pro 6.0 software (Photometrics).

Hormone analyses

Blood was collected at euthanasia *via* cardiac puncture with a syringe and needle precoated with heparin. Plasma was harvested by centrifugation (17,136 *g*, 10 min, 4°C) and stored at −20°C. The quantification of LH and follicle-stimulating hormone in mouse plasma was performed with the Milliplex Map Pituitary Magnetic Bead Panel Kit (PPTMAG-86K; MilliporeSigma, Burlington, MA, USA) according to the manufacturer's instructions. Samples were read on a Bio-Plex 200 suspension array system (Bio-Rad Laboratories, Hercules, CA, USA) with Bio-Plex Manager software (Bio-Rad Laboratories). To measure testosterone and corticosterone in mouse plasma, an isotope-dilution TurboFlow liquid chromatography–tandem mass spectrometry method was used, as previously described (34). Samples were analyzed in 7 batches. Each batch included standards for calibration curves, ~60 unknown samples, 1 blank, and control material prepared from a pool of human serum; 3 unspiked controls; 3 controls spiked at low levels; and 3 controls spiked at high levels. The interday variation, expressed as the relative SD for testosterone was 4.7 and 3.0% for low and high spike levels, respectively, and for corticosterone, the relative SD was 16.1 and 6.1% for low and high spike levels, respectively. The recovery was >89% for all analytes in both spike levels. Supplemental Table S1 shows the limit of quantification (34), the linear range for each individual calibration curve, and the interday validation. All chemical analyses were performed at the Department of Growth and Reproduction, Rigshospitalet, Copenhagen University Hospital.

Histology and immunostaining

For general histologic analysis, tissue sections were stained with hematoxylin and eosin (H&E), following standard protocols. Immunolocalization of a single protein was performed by a chromogenic immunostaining procedure, as previously described (35) whereas immunolocalization of 2 proteins on the same section was performed with a fluorogenic immunostaining procedure, as previously described (36). Antibodies used are detailed in **Table 2**. Images were captured using either an Axio Scan Z1 slide scanner (Carl Zeiss, Oberkochen, Germany) or an LSM 780 confocal microscope (Carl Zeiss).

Stereology

Leydig and Sertoli cells were identified in tissue sections by chromogenic immunostaining for HSD3B and SOX9, respectively. Quantification of cells was conducted with the stereology plugin for Image-Pro Plus 7.0 software (Media Cybernetics, Rockville, MD, USA) and a Zeiss Axio Imager A1 microscope fitted with a Qicam Fast 1394 digital camera (Qimaging, Surrey, BC, Canada) and a ProScan automated stage (Prior Scientific Instrument, Fulbourn, Cambridge, United Kingdom), as previously described (37). Briefly, the "count" function was used to score nuclei of immunopositive cells and to obtain the relative nuclear volume, which was then converted to absolute nuclear volume by testis weight. Mean nuclear volume was then measured with the "nucleator" function and used to calculate cell number/testis.

Seminiferous tubule diameter

Seminiferous tubule diameter was measured with the stereology plugin for Image-Pro plus 7.0 software and an Axio

TABLE 2. *Details of antibodies and detection methods used for chromogenic and fluorogenic immunostaining*

Target	Antigen retrieval	Primary antibody			Secondary reagent			Detection method
		Source	No.	Dilution	Source	No.	Dilution	
HSD3b	Citrate pH 6	Santa Cruz Biotechnology, Dallas, TX, USA	sc30820	1:2000	Vector Laboratories, Burlingame, CA, USA	MP-7405	NA	ImmPRESS HRP DAB
HSD3b	Citrate pH 6	Santa Cruz Biotechnology	sc30820	1:2000	Santa Cruz Biotechnology	sc-2961	1:200	ChαG HRP Tyramide
SOX9	Tris-EDTA pH 9	MilliporeSigma	AB5535	1:4000	Vector Laboratories	MP-7451	NA	ImmPRESS HRP DAB
SOX9	Tris-EDTA pH 9	MilliporeSigma	AB5535	1:4000	Vector Laboratories	PI-1000	1:200	GαR HRP Tyramide
RFP	n/a	Evrogen, Moscow, Russia	AB233	1:800	Vector Laboratories	BA-1000	1:500	Streptavidin HRP DAB
RFP	Citrate pH 6	Takara Bio, Kusatsu, Japan	632496	1:2000	Vector Laboratories	PI-1000	1:200	GαR HRP Tyramide
COUP-TFII	Citrate pH 6	Perseus Proteomics, Tokyo, Japan	PP-H7147-00	1:1000	Thermo Fisher Scientific	P0447	1:500	GαM HRP Tyramide
PDGFRb	Citrate pH 6	Abcam	ab32570	1:1500	Vector Laboratories	PI-1000	1:200	GαR HRP Tyramide

ChαG, chicken anti-goat; DAB, 3,3′-diaminobenzidine; GαM, goat anti-mouse; GαR, goat anti-rabbit; HRP, horseradish peroxidase; NA, not applicable.

Imager A1 microscope fitted with a Qicam Fast 1394 digital camera and a ProScan automated stage, as previously described (38).

Epididymal sperm reserve

The epididymal sperm reserves were quantified from frozen epididymides. The cauda epididymis was homogenized on ice in homogenization buffer (0.9% NaCl, 0.5% Triton X-100). Homogenization-resistant elongate spermatids were quantified with a hemocytometer.

Estimation of the proportion of LCs targeted by *Pdgfrb-Cre*

To determine the proportion of LCs targeted by the *Pdgfrb*-Cre, dual-fluorogenic immunostaining for HSD3B and RFP was performed. RFP^+;$HSD3B^+$ double-positive cells were counted and expressed as a percentage of total $HSD3B^+$ cells in a minimum of 10 images across 2 different testis sections from each of $n = 4$ animals.

Western blotting

Western blotting for CISD2 was performed, as previously described (39), with minor modifications. Briefly, 60 μg of protein was separated on an 8–16% Tris-glycine polyacrylamide gel (Thermo Fisher Scientific, Waltham, MA, USA) and transferred onto an Immobilon-Fl membrane (MilliporeSigma). Blots were probed with primary antibodies against CISD2 (13318-1-AP; 1:500; Proteintech, Rosemont, IL, USA) and glyceraldehyde-3-phosphate dehydrogenase (GAPDH; ab9483; 1:4000; Abcam, Cambridge, United Kingdom). Primary antibodies were detected with donkey anti-rabbit IRDye 800CW (925-32213, 1:10,000; Li-Cor Biosciences, Lincoln, NE, USA) and donkey anti-goat IRDye 680RD (925-68074; 1:10,000; Li-Cor Biosciences) secondary antibodies. Blots were imaged with the Odyssey imaging system (Li-Cor Biosciences).

Quantitative RT-PCR

Total RNA was extracted from frozen tissue with the RNeasy Mini Kit (Qiagen), per the manufacturer's instructions, including an on-column DNase (Qiagen) treatment step. An external control luciferase RNA (5 ng/testis; Promega, Madison, WI, USA) was added to each sample at the start of the extraction. RNA concentrations were determined with a NanoDrop 1000 v.3.8.1 spectrophotometer (Thermo Fisher Scientific). Random hexamer-primed cDNA was reverse transcribed from 2 μg total RNA with the SuperScriptVilo cDNA Synthesis Kit (Thermo Fisher Scientific), per the manufacturer's instructions. Real-time PCR was performed in 384-well format with the ABI Prism 7900HT Real-Time PCR System (Thermo Fisher Scientific) and the Universal ProbeLibrary (F. Hoffmann-La Roche, Basel, Switzerland). Assays were designed with the online Universal ProbeLibrary Assay Design Center tool (*https://lifescience.roche.com/en_gb/brands/universal-probe-library.html*). Details of each assay are listed in **Table 3**. The resulting data were analyzed using the cycle threshold $\Delta\Delta C_t$ method, with the expression of each gene related to the external luciferase control. The external luciferase control was assayed with forward, 5′-GCACATATCGAGGTGAACATCAC-3′ and reverse, 5′-GCCAACCGAACGGACATTT-3′, and, a 5′NED-labeled forward probe (5′-TACGCGGAATACTTC-3′).

Statistical analyses

Statistical analyses were performed with Prism 7.02 software (GraphPad Software, La Jolla, CA, USA). Data distribution was assessed by either the D'Agostino & Pearson or Shapiro-Wilk normality tests. Data were compared with either an unpaired, 2 tailed Student's t test or a Mann-Whitney U test as appropriate. Where required, data were normalized with the Box-Cox transformation using the optimal λ obtained from the online Free Statistics Software (v.1.2.1; *http://www.wessa.net/rwasp_boxcoxnorm.wasp/*). Inheritance of transgenes was assessed with a χ^2 test. In each case, a value of $P \leq 0.05$ was considered statistically significant.

TABLE 3. *Details of quantitative PCR assays*

Gene	Primer sequence, 5′–3′ Forward	Reverse	UPL probe
Lhcgr	GATGCACAGTGGCACCTTC	CCTGCAATTTGGTGGAAGAG	107
Star	AAACTCACTTGGCTGCTCAGTA	TGCGATAGGACCTGGTTGAT	83
Cyp11a1	AAGTATGGCCCCATTTACAGG	TGGGGTCCACGATGTAAACT	104
Hsd3b1	GAACTGCAGGAGGTCAGAGC	GCACTGGGCATCCAGAAT	12
Hsd3b6	ACCATCCTTCCACAGTTCTAGC	ACAGTGACCCTGGAGATGGT	95
Cyp17a1	CATCCCACACAAGGCTAACA	CAGTGCCCAGAGATTGATGA	67
Hsd17b3	AATATGTCACGATCGGAGCTG	GAAGGGATCCGGTTCAGAAT	5
Fshr	AGCCTTACCTACCCCAGTCAC	CAAATTGGATGAAGTTCAGAGGT	98
Inha	GGAAGATGTCTCCCAGGCTA	TGGCTGGTCCTCACAGGT	33
Inhbb	GGCAACCAGAACCTATTCGT	CATAGGGGAGCAGTTTCAGG	5

UPL, Universal ProbeLibrary.

RESULTS

KO of CISD2 in homozygous *Cisd2*$^{tm1a(EUCOMM)Wtsi}$ mice

To determine whether CISD2-deficient mice would provide a suitable platform to study age-related testicular dysfunction, we first confirmed the absence of CISD2 protein in *Cisd2*$^{tm1a(EUCOMM)Wtsi}$ mice. Heterozygous *Cisd2*$^{tm1a(EUCOMM)Wtsi}$ mice were intercrossed as described in Materials and Methods and genotyping primers designed around the synthetic cassette (**Fig. 1*A***) were used to identify WT, HET, and KO animals (Fig. 1*B*). The χ^2 analysis of offspring derived from heterozygous crossings confirmed that inheritance of WT and KO alleles conformed to predicted mendelian ratios (Fig. 1*C*). Western blotting on a panel of tissues, including liver and testis, confirmed absence of CISD2 protein in KO mice (Fig. 1*D*). Furthermore, growth curves from WT, HET, and HOM mice (Fig. 1*E*) revealed CISD2-deficient animals were significantly lighter from 8 wk of age compared with WT mice, consistent with previous reports of *Cisd2* disruption (29). We, therefore, concluded that the KO-first *Cisd2*$^{tm1a(EUCOMM)Wtsi}$ allele functioned as expected (a null allele) and that CISD2 loss associated with that allele was functionally significant.

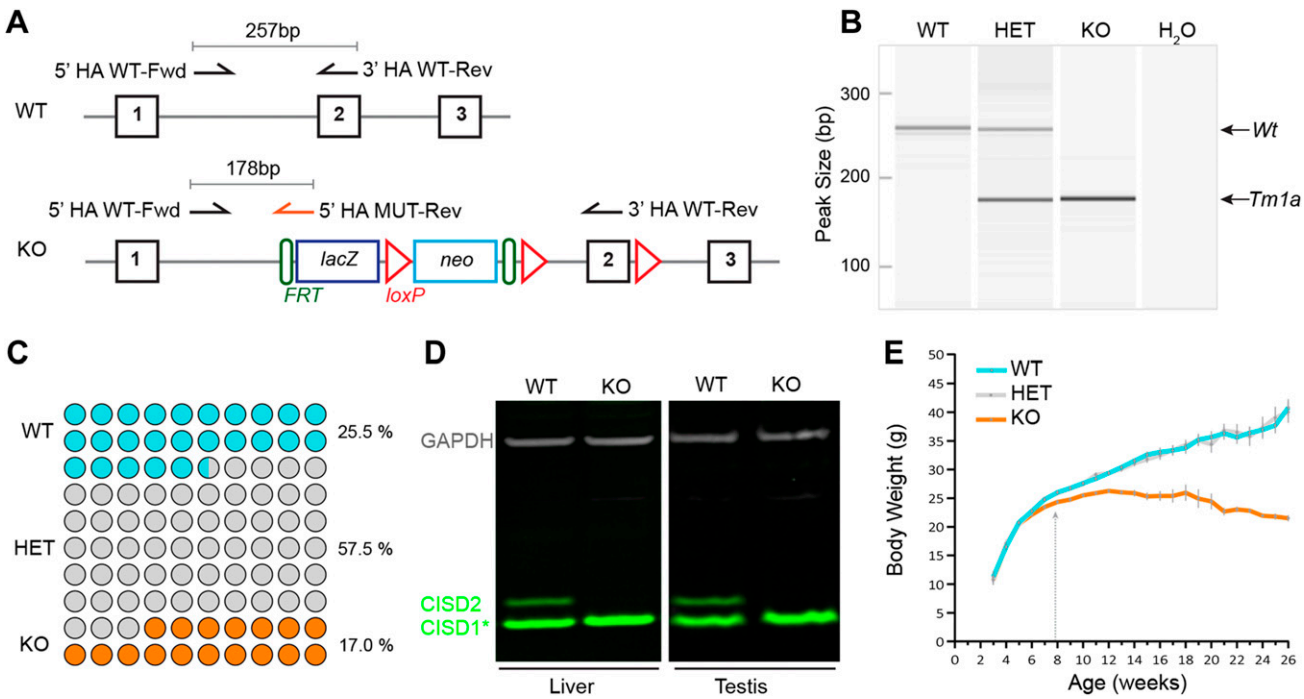

Figure 1. Validation of the knockout-first *Cisd2* allele. *A*) Schematic of the WT and KO-first alleles detailing the location of genotyping primers and expected size of PCR products. *B*) PCR analysis of genomic DNA isolated from ear clips of WT (257 bp), HET (257 and 178 bp), and homozygous (KO; 178 bp) mice. *C*) Inheritance of WT and KO alleles in offspring derived from heterozygous crossings conformed to predicted Mendelian ratios (χ^2; $P = 0.4224$), with no gender bias. *D*) Western blot analysis of liver and testis confirmed CISD2 protein was absent in KO mice. The lower band is predicted to be CISD1 based on the size and sequence homology in the region of the protein that the antibody was raised against. *E*) Growth curves of WT, HET, and KO mice revealed CISD2-deficient animals were significantly lighter from 8 wk of age compared with WT animals [$P = 0.003691$ at 8 wk, $P = 0.000419$ at 26 wk (WT *vs.* KO individual Student's *t* test; $n = \geq 5$ animals/genotype/time point)]. Values are means ± SEM.

Testicular atrophy in CISD2-deficient mice

Having validated ablation of CISD2 in KO animals, we next sought to assess the effect of CISD2 deficiency (and, by inference, premature aging) on testicular architecture. No overt dysmorphology of the reproductive tract was noted, although testes and seminal vesicles appeared slightly smaller in KO animals (**Fig. 2*A***). In addition, a striking reduction in epididymal fat pad mass was apparent in the KO mice, in line with the previously reported (40) requirement of CISD2 for normal adipogenesis. Indeed, testis weight was significantly reduced in KO mice compared with WT controls (Fig. 2*B*). Although testicular histology was largely normal in KO mice, with abundant interstitial LCs and full spermatogenesis occurring within seminiferous tubules, degenerating tubules were occasionally noted (Fig. 2*C*).

Given that the structure and function of the seminiferous tubules is entirely dependent on the SC population (35, 41), we next asked whether the tubular degeneration in the KO testis could be explained by a deficit in this cell population. Immunoreactivity of the SC marker SOX9 was observed, as expected, around the periphery of the seminiferous tubules in WT and KO testes (**Fig. 3*A***). However, stereologic analysis revealed a significant reduction in SC number in the KO testis compared with WT controls (Fig. 3*B*). This decrease in the SC population was associated with a significant reduction in the diameter of the seminiferous tubules (Fig. 3*C*) and a reduction in the epididymal sperm reserve (Fig. 3*D*) in KO mice. Circulating follicle-stimulating hormone (Fig. 3*E*) and testicular mRNA expression of *Fshr*, *Inha*, and *Inhbb* (Fig. 3*F*, *G*) were similar between WT and KO animals. Taken together, these observations suggest CISD2 loss results in premature focal testicular atrophy consistent with age-related testicular atrophy observed in both rodents and humans (42–50).

Testicular endocrine dysfunction resembling compensated LC failure in CISD2-deficient mice

In addition to atrophy of the seminiferous tubules, aging is associated with a reduction in LC androgen biosynthesis. As such, we next asked whether LC number or function was altered in prematurely aging CISD2-deficient mice. As expected, immunoreactivity of the LC marker HSD3B was observed in the interstitial compartment in WT and KO testes (**Fig. 4*A***). However, when quantified, a significant reduction in LC number was observed in KO mice compared with WT controls (Fig. 4*B*). Next, we assessed whether LC function was compromised in the KO testis. Total circulating plasma testosterone and seminal vesicle weight (as a biomarker of peripheral androgen action) were both reduced in KO mice compared with WT controls (Fig. 4*C*, *D*, respectively). Importantly, the reduction in circulating testosterone could not be attributed simply to reduced LC numbers because circulating plasma testosterone relative to LC number was also reduced in KO mice (Fig. 4*E*). No significant difference in circulating LH was noted between WT and KO animals (Fig. 4*F*). However, the LH, luteinizing hormone to testosterone (LH/T) ratio was significantly distorted (Fig. 4*G*), indicative of compensated LC failure. Additionally, mRNAs of key LC-expressed genes required for the conversion of cholesterol to testosterone were significantly decreased in KO testes (**Fig. 5**), consistent with age-related LC dysfunction (17, 18, 20). Together, those observations point toward primary LC dysfunction in KO mice and suggest that the CISD2-KO mouse has utility as a model of the premature aging of the male reproductive system.

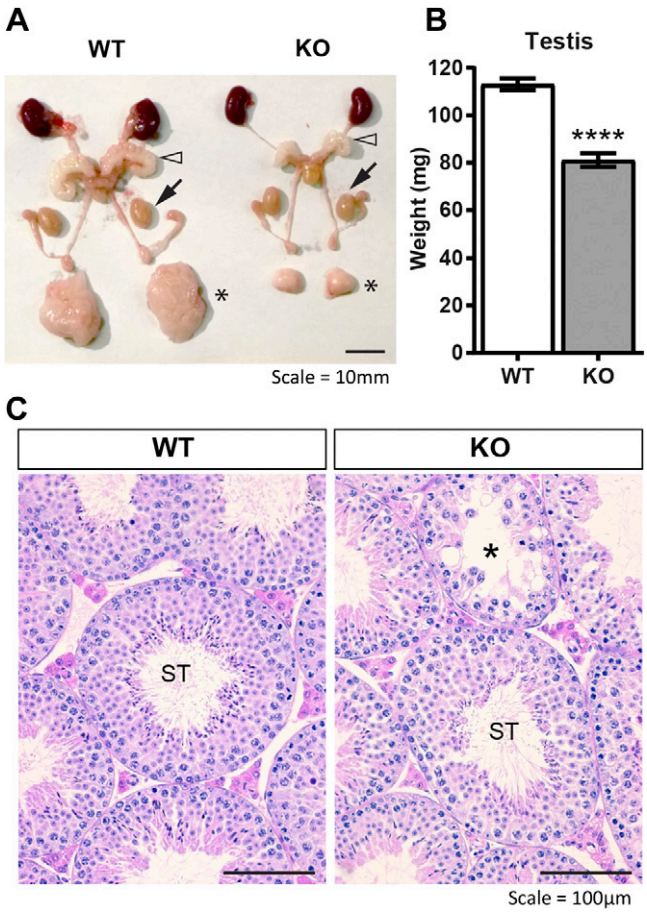

Figure 2. Testis weight is reduced in CISD2-deficient mice. *A*) Representative reproductive tracts from WT and KO mice at ~6 mo of age. Open arrowheads, seminal vesicle; closed arrows, testis. Note the striking reduction in epididymal fat-pad mass (asterisks). Scale bar, 10 mm. *B*) A significant reduction in testis weight was observed in KO mice compared with WT controls. ****$P = <0.0001$, unpaired Student's t test; $n = 9$–10). Error bars = SEM. *C*) H&E–stained testis sections from WT and KO mice. In each case, abundant interstitial LCs and seminiferous tubules (ST) with full spermatogenesis were present. However, occasional degenerating tubules (asterisks) were noted in the KO testis. Scale bars, 100 μm.

Generation of LC- and SC-specific *Cisd2*-KO mice

To better understand the cause and effect relationship between aging and declining testosterone levels, we next sought to separate the effects of aging in

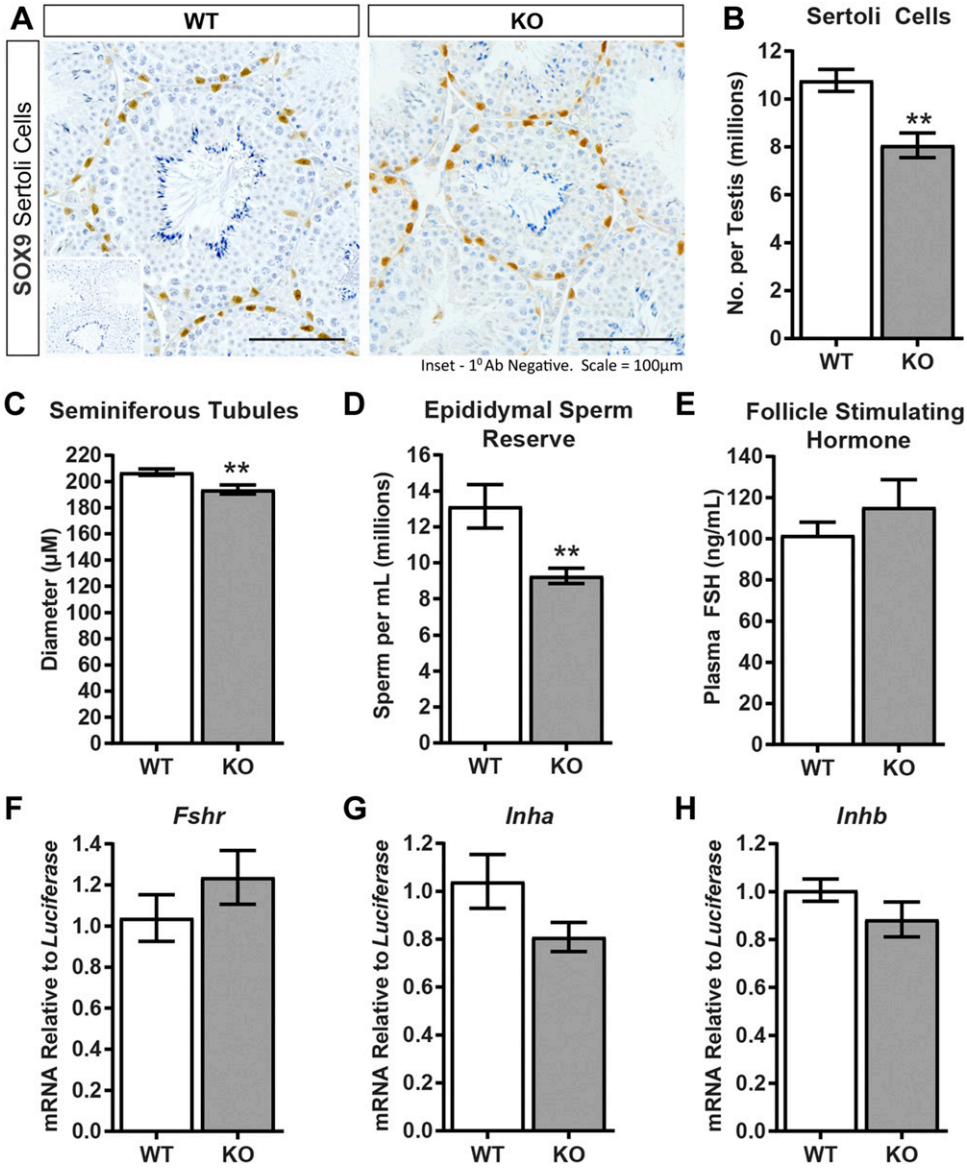

Figure 3. SC number, seminiferous tubule diameter, and epididymal sperm reserves are reduced in CISD2-deficient mice up to 6 mo of age. *A*) Representative chromogenic immunostaining of the SC marker SOX9 (SRY-Box 9) in WT and KO testes. *B*) SC number was reduced in KO testes compared with WT controls. $^{**}P = 0.0016$ (unpaired Student's *t* test; $n = 8$). *C*) Seminiferous tubule diameter was significantly reduced in KO mice compared with WT controls. $^{**}P = 0.0033$, (Mann Whitney *U* test; $n = 8$). *D*) Epididymal sperm reserves were significantly reduced in KO mice compared with WT controls. $^{**}P = 0.0091$ (unpaired Student's *t* test; $n = 8$). *E*) Circulating follicle-stimulating hormone was similar between WT and KO mice ($P = 0.3700$, Student's *t* test; $n = 11$–12). *F*–*H*) Testicular mRNA expression of follicle stimulating hormone receptor (*Fshr*) (*F*), inhibin subunit α (*Inha*) (*G*) and inhibin subunit β (*Inhbb*) (*H*) was similar between WT and KO mice [$P = 0.2801$, $P = 0.0816$, and $P = 0.1931$, respectively (Student's *t* test; $n = 7$–8)]. Error bars = SEM.

the testis from systemic aging. First, to determine whether LC dysfunction in constitutive CISD2-KO mice was due to specific effects of premature aging intrinsic to LCs, we used *Cisd2*$^{tm1c(EUCOMM)Wtsi}$ to disrupt *Cisd2* in LCs. Additionally, because SCs have an important paracrine role in the retention of the adult LC population (35, 51), we also disrupted SC *Cisd2* to determine whether premature aging in SCs affects LC function. We first assessed the utility of *Pdgfrb*-Cre mice in targeting the adult LC population. *Pdgfrb*-Cre mice were bred to tdTomato Cre-reporter mice as described in Materials and Methods. Dual fluorescent immunohistochemistry for RFP and HSD3B revealed colocalization in ~55% of LCs in the adult testis (**Fig. 6*A***). RFP expression was also observed in peritubular and perivascular cells as well as in a subpopulation of SCs. As the population of LCs in the adult testis developed from a pool of peritubular and/or perivascular stem/progenitor cells during pubertal development (52–59), we further demonstrated that the *Pdgfrb*-Cre targets adult LCs from the stem/progenitor stage in fetal life (Supplemental Fig. S2). We also confirmed SC-specific activity of Amh-Cre in RFP reporter mice by dual-fluorescent immunohistochemistry for RFP and SOX9. As expected, Cre expression was confined to testicular SCs as evidenced by the pattern of RFP-positive staining, characteristic of SC cytoplasm, in cells positive for the SC nuclear marker SOX9 (Fig. 6*B*). Having demonstrated LC and SC targeting with *Pdgfrb*-Cre and *Amh*-Cre lines, respectively, we next generated LC and SC *Cisd2*-KO mice, as described in the Materials and Methods (referred to as LC-KO and SC-KO, respectively, hereafter). PCR interrogation of testicular genomic DNA isolated from testes of LC-KO, SC-KO, and their respective WT controls confirmed recombination of the conditional *Cisd2* allele in the presence of either Cre recombinase (Fig. 6*C*).

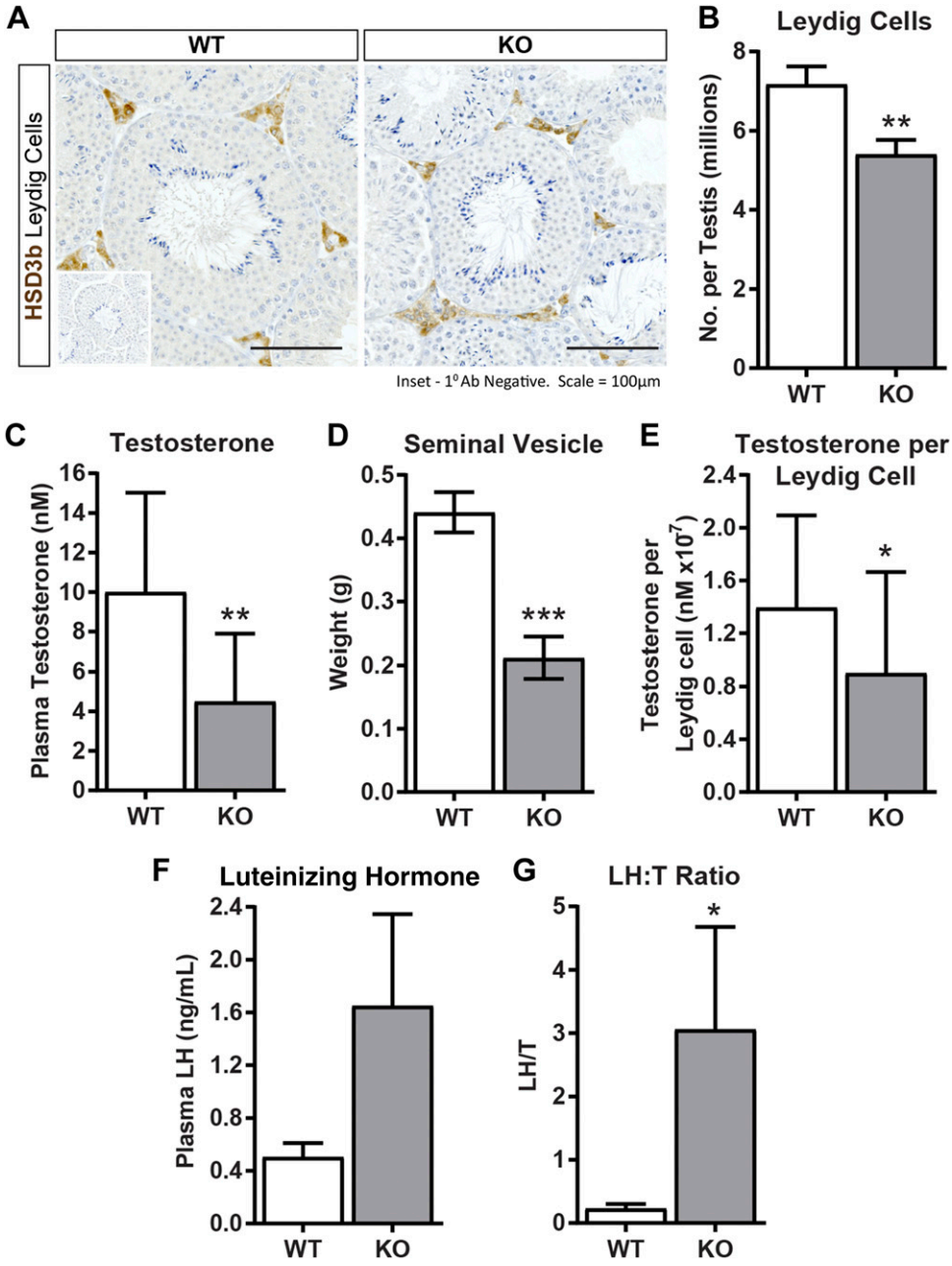

Figure 4. LC number and circulating testosterone are reduced in CISD2-deficient mice up to 6 mo of age. *A*) Representative chromogenic immunostaining of the LC marker hydroxysteroid dehydrogenase 3-β (HSD3B) in WT and KO testes. Scale bars, 100 µm. *B*) LC number was significantly reduced in KO mice compared with WT controls (unpaired Student's *t* test; $n = 8$). $^{**}P = 0.0085$. *C*, *D*) Both total circulating testosterone (*C*) and seminal vesicle weight (*D*), as biomarker of peripheral androgen action, were significantly reduced in KO mice. $^{**}P = 0.0085$ (Student's *t* test; $n = 12$), $^{***}P = 0.0010$ (Mann Whitney *U* test; $n = 9$–10). *E*) Circulating testosterone relative to LC number was also reduced in KO mice compared with WT controls. $^{*}P = 0.0280$ (unpaired Student's *t* test; $n = 12$). *F*) No difference in circulating luteinizing hormone was observed between WT and KO mice ($P = 0.2215$, unpaired Student's *t* test; $n = 10$–12). *G*) The luteinizing hormone/testosterone ratio was significantly increased in KO mice compared with WT controls ($P = 0.0232$, unpaired Student's *t* test; $n = 10$–12). Error bars = SEM.

Disruption of *Cisd2* in either LCs or SCs does not result in premature testicular dysfunction

In contrast to the phenotype observed in constitutive CISD2-KO animals in which body weight was significantly reduced from 8 wk of age (Fig. 1*E*), body weight was maintained in LC-KO and SC-KO animals (**Fig. 7*A***). In fact, an increase in body weight was observed in LC-KO animals. Because testicular atrophy accompanied by decreased SC number, seminiferous tubule diameter, and epididymal sperm reserves was observed in constitutive-KO testes (Figs. 2*B*, *C* and 3*B*–*D*), we next asked whether that phenotype was recapitulated when *Cisd2* was disrupted in either LCs or SCs alone. Testis weight was within reference range in both LC-KO and SC-KO animals (Fig. 7*B*), with no histologic evidence of tubular degeneration (Fig. 7*C*) as noted in constitutive-KO animals (Fig. 2*C*). Additionally, SC number (**Fig. 8*A*, *B***), tubule diameter (Fig. 8*C*), and epididymal sperm reserves (Fig. 8*D*), as well as circulating follicle-stimulating hormone (Fig. 8*E*) and testicular *Fshr*, *Inha*, and *Inhbb* mRNA expression (Fig. 8*F*, *G*) were similar between LC-KO, SC-KO, and their respective controls. Taken together, these observations suggest that neither LCs nor SCs alone are responsible for the degenerative testicular phenotype observed in constitutive-KO animals.

We next asked whether LC dysfunction observed in constitutive CISD2-KO animals (Figs. 4 and 5) was a direct consequence of CISD2 loss from the LC population or was due to indirect paracrine effects mediated by SC dysfunction. LC number, circulating testosterone, and seminal vesicle weight were normal in both in LC-KO and in SC-KO mice compared with their respective WT controls

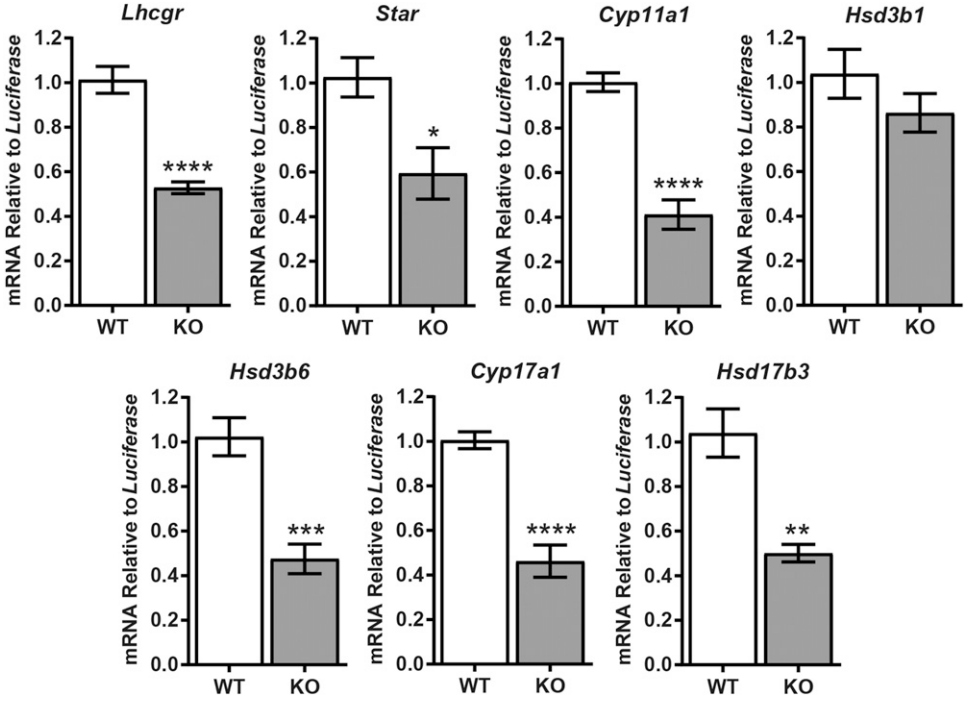

Figure 5. Steroidogenic gene expression is altered in CISD2-deficient testes. Testicular mRNA expression of genes involved in LC testosterone biosynthesis was reduced in KO mice compared with WT controls at ~6 mo of age. Luteinizing hormone/chorionic gonadotropin receptor (*Lhcgr*), $^{****}P = 0.0001$; steroidogenic acute regulatory protein (*Star*), $^{*}P = 0.0102$; P450 cholesterol side-chain cleavage enzyme (*Cyp11a1*), $^{****}P < 0.0001$; hydroxysteroid dehydrogenase 3-β type 1 (*Hsd3b1*), $P = 0.2309$; hydroxysteroid dehydrogenase 3-β type 6 (*Hsd3b6*), $^{***}P = 0.0002$; 17α-hydroxylase, 17,20-lyase (*Cyp17a1*), $^{****}P = <0.0001$; and hydroxysteroid dehydrogenase 17-β type 3 (*Hsd17b3*), $^{**}P = 0.0012$ (unpaired Student's *t* tests; $n = 8$). Error bars = SEM.

(**Fig. 9*A–D***). To determine whether circulating testosterone levels are maintained through functional compensation by the remaining 45% WT LCs in the LC-KO testis (*i.e.*, those not targeted by the *Pdgfrb*-Cre; Fig. 6*A*), mice were injected with hCG (an LHCGR agonist) to stimulate maximal LC testosterone production. However, no difference in hCG-stimulated testosterone was observed (Fig. 9*E*), effectively ruling that possibility out. In addition, no difference in circulating LH (Fig. 9*F*), the LH/T ratio (Fig. 9*G*), or testicular expression of steroidogenic mRNAs (**Fig. 10**) was detected in LC-KO or SC-KO mice compared with their respective controls, suggesting that LC steroidogenic function is maintained when *Cisd2* is disrupted either in LCs or SCs alone. Taken together, these data demonstrate that the mechanisms underlying the primary testicular failure observed in prematurely aged constitutive CISD2-KO animals cannot be assigned to specific dysfunction of the LC or SC populations alone.

Alterations in the wider endocrine milieu during aging may affect LC function. Circulating glucocorticoids are reported to increase in aging rats and humans (60–62), and the suppressive effects of glucocorticoids on testosterone production are well documented (63–69). With this in mind, we next assessed circulating corticosterone levels and found a significant increase in constitutive CISD2-KO mice, whereas levels were unchanged in both LC-KO and SC-KO mice (**Fig. 11*A***). Furthermore, testicular mRNA expression of *Nr3c1*, encoding the glucocorticoid receptor, which was previously reported to be under autoregulation (70, 71), was significantly decreased in constitutive-KO mice (Fig. 11*B*). Additionally, although testicular mRNA expression *Hsd11b1* was similar between constitutive and conditional KO mice and their respective controls, expression of *Hsd11b2* was decreased in the constitutive KOs, potentially indicating a perturbation in intercellular glucocorticoid metabolism (Fig. 11*C*, *D*).

DISCUSSION

Aging in men is accompanied by a decline in testicular function. Of particular importance is the reported age-related decrease in the endocrine function of the testis (*e.g.*, androgen production) (3–7, 14) because an inverse relationship between circulating testosterone levels and cardiometabolic disease risk has been suggested (8–12). However, the cause–consequence relationship between androgens, aging, and disease is unclear. Specifically, the precise mechanisms by which LC testosterone production becomes compromised, leading to age-related primary hypogonadism, remains to be established. Using a series of novel mouse models of premature aging, we now demonstrate that age-related testicular atrophy and LC dysfunction are not entirely explained by intrinsic aging in either LCs or SCs *per se*. Instead, we suggest that aging-induced disruption to the testicular microenvironment and/or wider systemic effects of aging may be significant contributing factors to age-related testicular dysfunction.

Age-related testicular atrophy is well documented both in humans and in rodents. Testicular volume declines with advancing age and is linked to a reduction in SC number and/or function, involution of the seminiferous tubules, and diminished spermatogenesis (42–49, 72–74). Consistent with that, our histomorphometric analyses of constitutive CISD2-KO mice revealed a testicular phenotype characterized by reduced testis weight, seminiferous

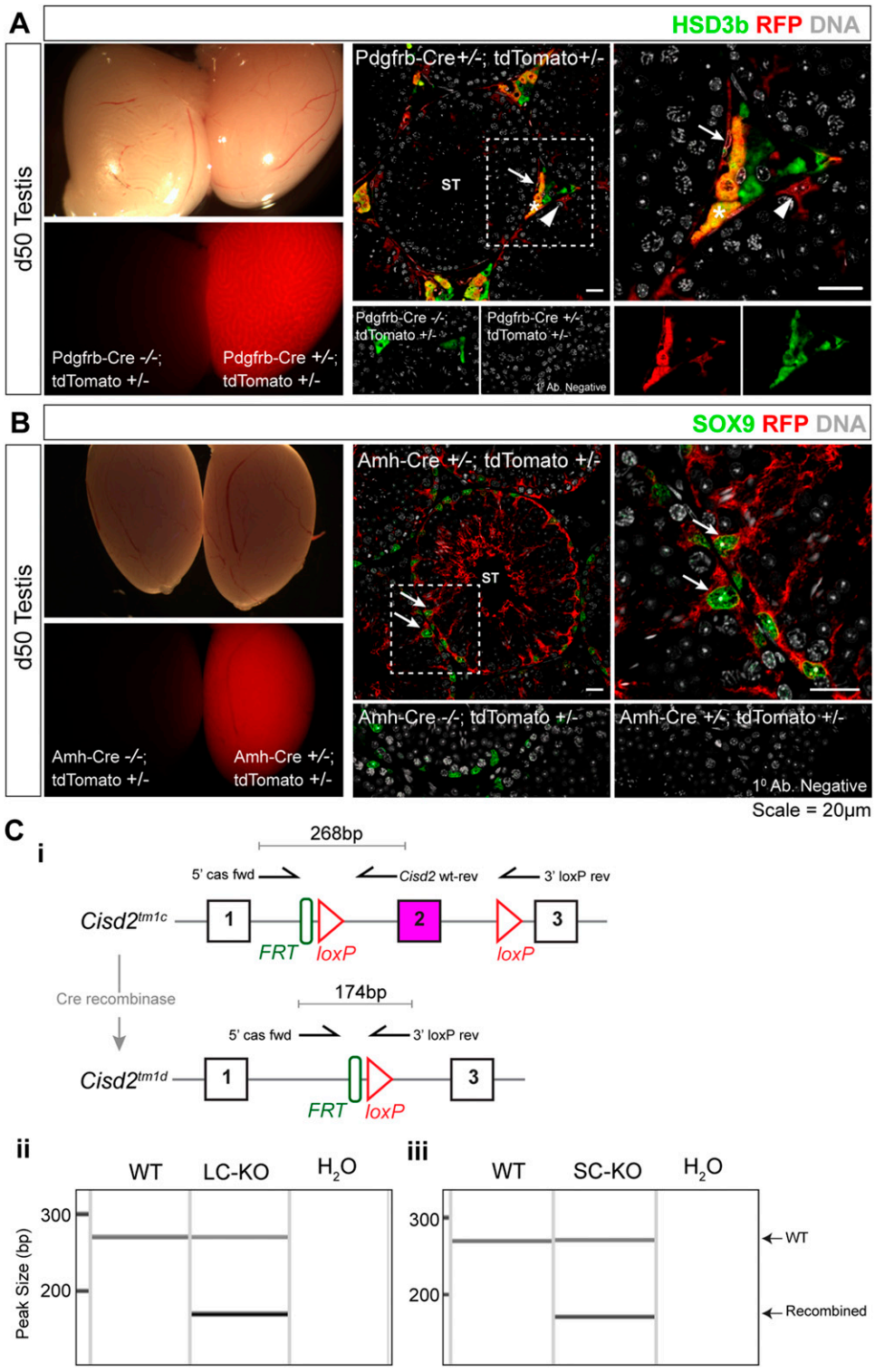

Figure 6. Generation of LC- and SC-specific *Cisd2*-KO mice. *A*) Analysis of *Pdgfrb*-Cre activity in the testis young adult tdTomato Cre-reporter mice. Coimmunostaining of RFP with the LC marker HSD3B revealed that Cre-recombinase is active in ~55 ± 3.9% (mean ± SEM) of adult LCs. Expression was also observed in the peritubular cells (arrows) as well as in a proportion of SCs (closed arrowheads). Scale bar, 20 µm. *B*) Confirmation of SC-specific targeting with *Amh*-Cre. Coimmunostaining of RFP with the SC marker SOX9 showed RFP expression was restricted to SCs. *C*) Schematic of the conditional *Tm1c* allele detailing the location of genotyping primers and expected size of PCR products following Cre-mediated recombination (*i*). PCR analysis of testicular genomic DNA confirmed the conditional *Cisd2* allele was recombined upon exposure to either *Pdgfrb*-Cre (LC-KO) (*ii*) or *Amh*-Cre (SC-KO) (*iii*). WT = 268 bp; KO (recombined) = 174 bp.

tubule diameter, SC number, and epididymal sperm reserves. Significantly, in comparison with previous reports of aging in the rodent testis, signs of age-related atrophy in constitutive CISD2-KO mice are observed ~18 mo earlier than in naturally aged animals (43–45). As such, prematurely aging CISD2-KO mice provide a valuable platform for the expedited study of aging in the testis.

Testicular endocrine function (*i.e.*, testosterone production) also deteriorates during the aging process, which may be attributed to either a defect in LC androgen biosynthesis (primary hypogonadism) or to reduced stimulation of LCs because of decreased hypothalamic–pituitary LH secretion (secondary hypogonadism). The latter has been associated with obesity in men (75), and its prevalence is not reported to increase with advancing age (76). Instead, progressive, age-related reduction in testosterone level is thought to be predominantly caused by primary testicular dysfunction (14, 76, 77). It has been reported that

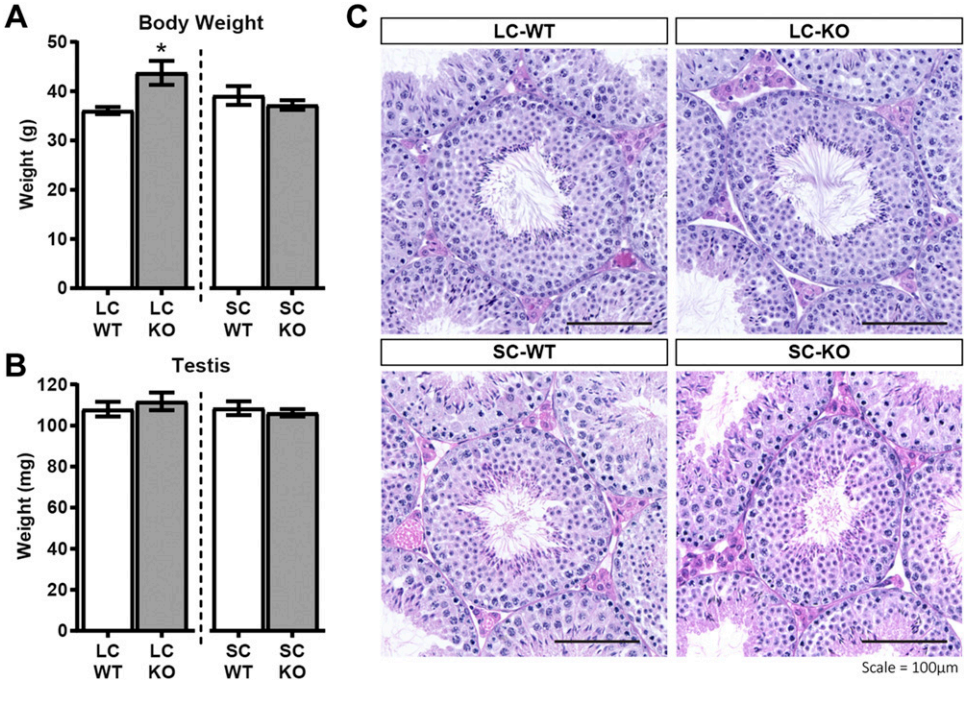

Figure 7. Testis weight is unaltered when *Cisd2* is disrupted either in LCs or in SCs. *A*) Contrary to the phenotype observed in constitutive CISD2-KO mice, body weight was not reduced either in LC-KO (left) or in SC-KO (right) animals at 6 mo of age. In fact, an increase in body weight was noted in LC-KO animals compared with LC-WT controls. **P* = 0.0166 [SC-WT *vs.* SC-KO, *P* = 0.3688 (unpaired Student's *t* test; *n* = 7–8)]. *B*) No difference in testis weight was observed between LC-KO or SC-KO mice and their respective WT controls [LC-WT *vs.* LC-KO, *P* = 0.5126l SC-WT *vs.* SC-KO, *P* = 0.5382 (unpaired Student's *t* test; *n* = 7–8)]. Error bars = SEM. *C*) Representative H&E stained testis sections of LC-KO (top) and SC-KO (bottom) mice and their respective WT controls. Testicular architecture remained normal when *Cisd2* was disrupted in either LCs or SCs. Scale bars, 100 µm.

testosterone levels decrease in aging mice because of reduced frequency and amplitude of LH pulses (*i.e.*, secondary hypogonadism) (78, 79). Conversely, others have reported that LH and testosterone levels remain stable up to 31 mo of age in mice (80, 81). As such, naturally aged mice may be refractory to age-related LC dysfunction, potentially limiting their utility as a model of human primary hypogonadism. The ratio of luteinizing hormone to testosterone is a well-established indicator of LC function, with an increased ratio indicative of primary LC dysfunction. In the present studies, we noted a reduction in total circulating testosterone accompanied by an increase in the LH/testosterone ratio in constitutive CISD2-KO mice, consistent with age-related primary hypogonadism in aging men. This phenotype was not recapitulated when *Cisd2* disruption (and by inference premature aging) was restricted to LCs, suggesting that the otherwise young testicular microenvironment in this conditional model is conducive to testosterone production by prematurely aged LCs.

Interestingly, when healthy and diseased aged mice are considered separately, a reduction in circulating testosterone is reported in diseased mice (82). However, as circulating gonadotropins were not measured in that study, it is not known whether the hypogonadism in the aged, diseased animals was primary or secondary in nature. Additionally, the cross-sectional nature of the study prevents any interpretation of causality (*i.e.*, whether low testosterone levels drive disease progression or *vice versa*). In line with previous studies by Chen *et al.* (29) and Wang *et al.* (40), the CISD2-KO mice described herein had a marked reduction in adipose tissue. Although resection of the epididymal white adipose tissue depot has been shown to have a negative effect on spermatogenesis, circulating testosterone and LH are unaffected (83). As such, we suggest that prematurely aging CISD2-KO mice represent a novel model for the study of age-related primary hypogonadism, without confounding issues associated with increased adiposity and associated hypothalamic/pituitary dysfunction observed in naturally aged animals.

In humans, circulating testosterone is either specifically bound to sex hormone binding globulin (SHBG), weakly bound to albumin, or is not associated with binding proteins (*i.e.*, is free) (84, 85). SHBG is primarily produced by the human liver, whereas in rodents, the equivalent, androgen binding protein (ABP), is produced by testicular SCs (86–88). In aging men, SHBG levels increase, contributing to reduced free circulating testosterone (6), which represents an additional layer of complexity in the progression of age-related hypogonadism. Whether ABP levels are altered in aging rodents is unclear, but it is possible that species differences in steroid binding proteins, particularly very low levels/absence of ABP in the mouse compared with the rat (87), may partially explain why naturally aged mice do not fully model human age-related primary hypogonadism. This requires further study.

Testosterone deficiency may be attributed to reduced number and/or function of LCs. Early studies reported up to a 44% reduction in LC numbers in the aging human testis, accompanied by a 2-fold increase in LH to maintain circulating testosterone levels (89–91). However, a more-recent study reported decreased numbers of SCs, but not LCs in the aging human testis (92). In the brown Norway rat, LC number is maintained in aged animals, whereas steroidogenic

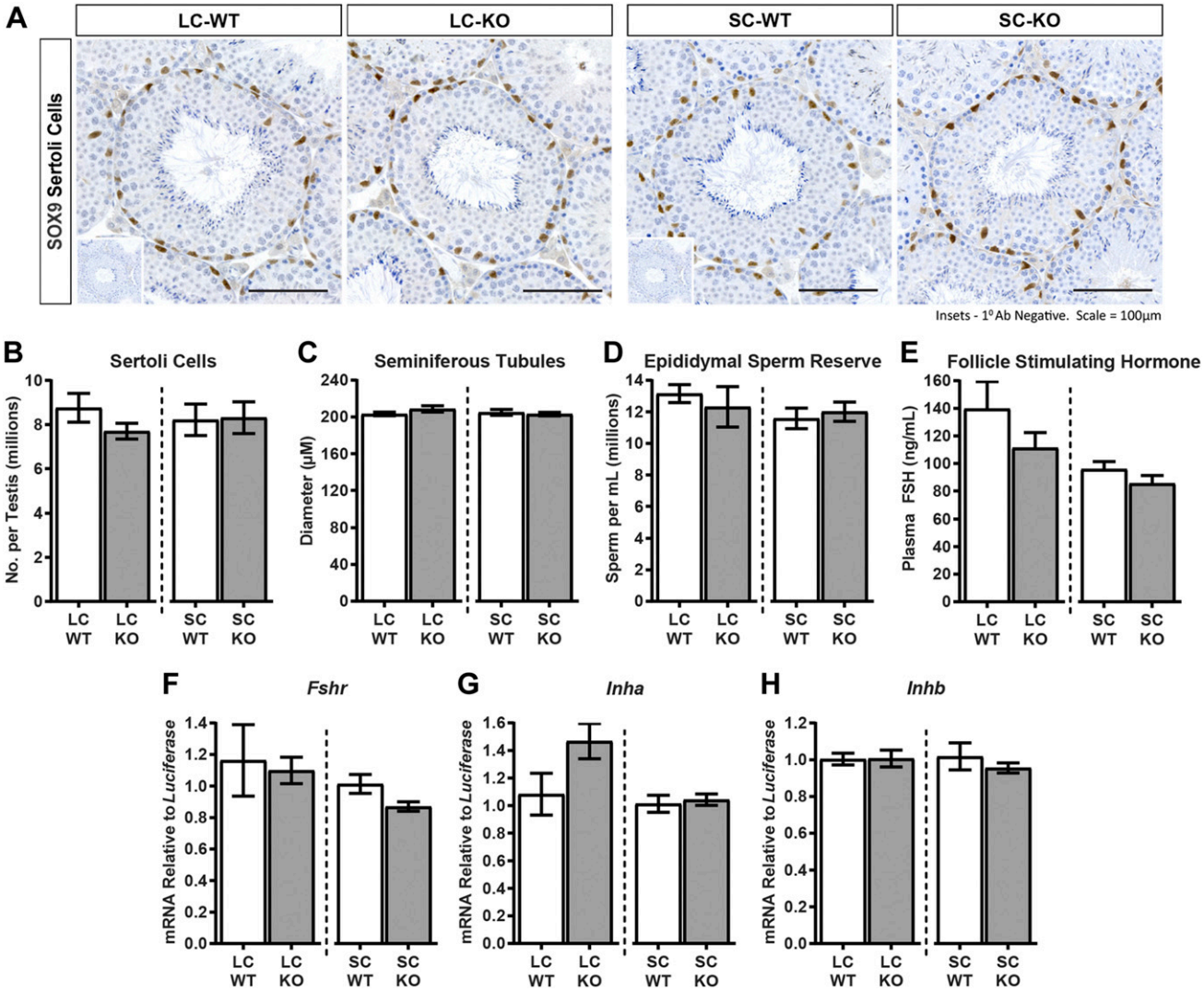

Figure 8. SC number, seminiferous tubule diameter, and epididymal sperm reserves are maintained when *Cisd2* is disrupted in LCs or SCs. *A*) Representative chromogenic immunostaining of the SC marker SOX9 in 6-mo-old LC-KO and SC-KO testes. *B*) SC numbers were maintained in LC-KO and SC-KO testes when compared with their respective WT controls [LC-WT *vs.* LC-KO, $P = 0.1604$; SC-WT *vs.* SC-KO, $P = 0.9264$ (unpaired Student's *t* test; $n = 7–9$)]. *C, D*) No difference in seminiferous tubule diameter (*C*) [LC-WT *vs.* LC-KO, $P = 0.1736$; SC-WT *vs.* SC-KO, $P = 0.6188$ (unpaired Student's *t* test; $n = 7–8$)] or epididymal sperm reserve (*D*) [LC-WT *vs.* LC-KO, $P = 0.5625$; SC-WT *vs.* SC-KO, $P = 0.6429$ (unpaired Student's *t* test; $n = 6–8$)] was noted in LC-KO or SC-KO mice compared with their respective WT controls. *E*) Circulating follicle-stimulating hormone was unaltered both in LC-KO and in SC-KO mice [LC-WT *vs.* LC-KO, $P = 0.2303$; SC-WT *vs.* SC-KO, $P = 0.2024$ (unpaired Student's *t* test; $n = 8–11$)]. *G, H*) No difference in testicular mRNA expression of follicle-stimulating hormone receptor (*F*) (*Fshr*) [LC-WT *vs.* LC-KO, $P = 0.7971$; SC-WT *vs.* SC-KO, $P = 0.0507$ (Student's *t* test; $n = 8$)], inhibin subunit α (*Inhα*, *G*) [LC-WT *vs.* LC-KO, $P = 0.0736$; SC-WT *vs.* SC-KO, $P = 0.6970$ (Student's *t* test; $n = 8$)], or inhibin subunit β (*Inhbb*, *H*) 9 LC-WT *vs.* LC-KO, ns $P = 0.9582$; SC-WT *vs.* SC-KO, $P = 0.4391$ (unpaired Student's *t* test; $n = 8$)], and LC-KO, SC-KO, and their respective controls were similar. Error bars = SEM.

function is reduced, in part, because of reduced expression of genes required for testosterone biosynthesis (93, 94). In the present studies, we report a reduction in the number of LCs in prematurely aging CISD2-KO mice. Additionally, mRNA expression of genes required for LC androgen biosynthesis was reduced in constitutive CISD2-KO animals. This could potentially limit the capacity for increased steroidogenic flux to maintain normal testosterone levels in the face of reduced LC number. For example, in other rodent models, with up to a 75% reduction in LC number, testosterone levels are maintained because of functional compensation by the remaining LC population (35, 41, 95). Indeed, reduced circulating testosterone in constitutive CISD2-KO animals was not entirely explained by correction for the reduction in LC number, confirming a primary LC dysfunction in this model. Surprisingly, LC number and function were maintained in conditional LC-KO and in SC-KO mice, suggesting that impaired LC function in constitutive KO mice is not explained by aging specifically in either LCs or SCs alone.

In addition to reduced expression and activity of proteins required for the conversion of cholesterol to

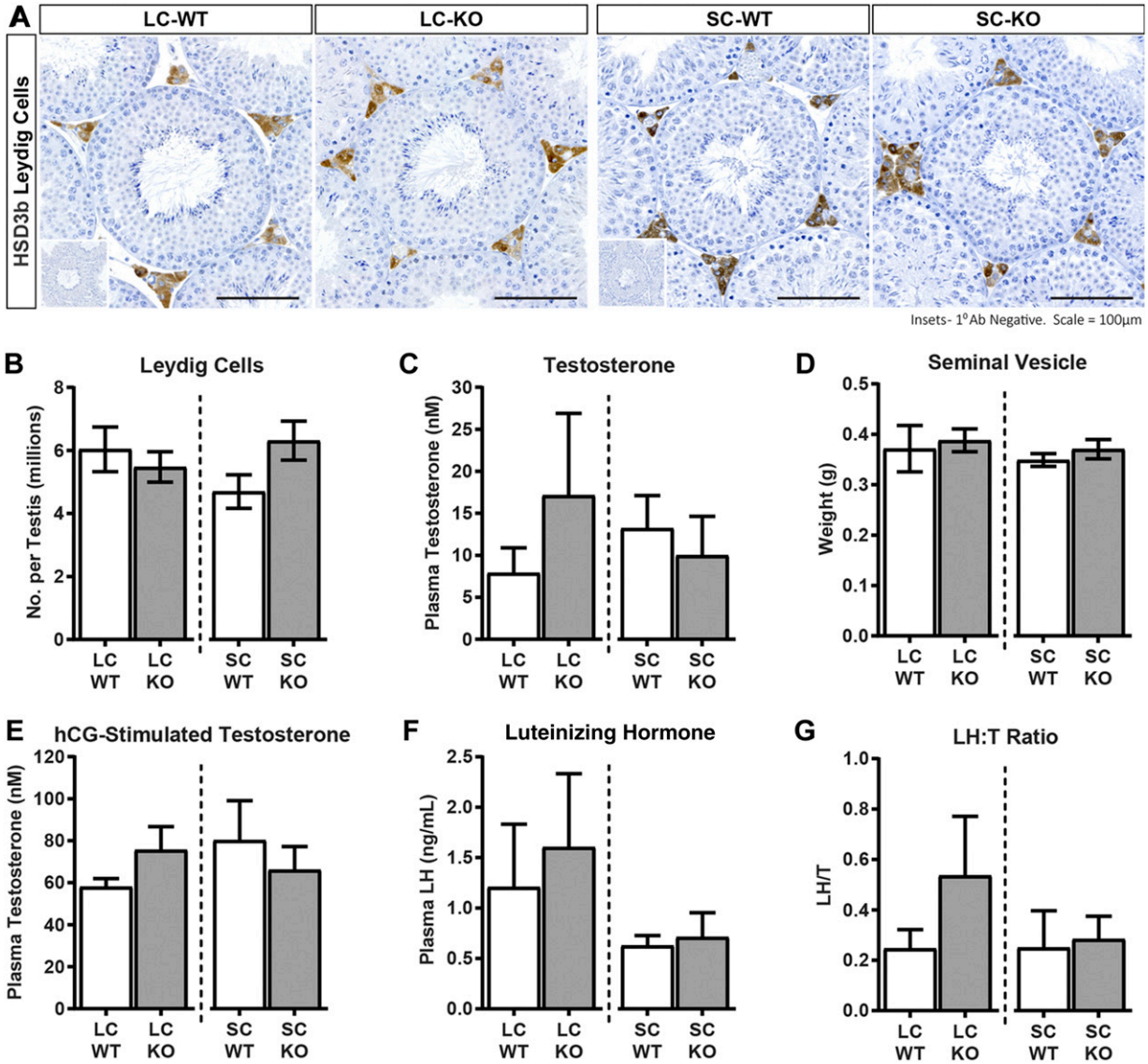

Figure 9. Circulating testosterone is maintained when *Cisd2* is disrupted either in LCs or in SCs. *A*) Representative chromogenic immunostaining of the LC marker HSD3B in 6-mo-old LC-KO, SC-KO, and control testes. *B*) Stereologic analysis revealed that LC number was normal in LC-KO and SC-KO testes compared with their respective controls (unpaired *t*-tests, LC-WT *vs.* LC-KO, $P = 0.5158$; SC-WT *vs.* SC-KO, $P = 0.0736$; $n = 7–9$). *C*) Circulating testosterone was normal in LC-KO and SC-KO mice compared with their respective controls [LC-WT *vs.* LC-KO, $P = 0.9325$; SC-WT *vs.* SC-KO, $P = 0.2827$ (unpaired Student's *t* test; $n = 8–11$)]. *D*) Weight of the androgen-dependent seminal vesicle was maintained in LC-KO and SC-KO mice [LC-WT *vs.* LC-KO, $P = 0.3823$; SC-WT *vs.* SC-KO, $P = 0.3843$ Mann Whitney *U* test and unpaired Student's *t* test, respectively; $n = 8–11$)]. *E*) LC response to maximally stimulating hCG was normal in both LC-KO and SC-KO mice [LC-WT *vs.* LC-KO, $P = 0.1869$; SC-WT *vs.* SC-KO, $P = 0.5177$ (unpaired Student's *t* test; $n = 4–6$)]. *F*) Circulating luteinizing hormone was normal in both LC-KO and SC-KO mice [LC-WT *vs.* LC-KO, $P = 0.3817$; SC-WT *vs.* SC-KO, $P = 0.8225$ (unpaired Student's *t* test; $n = 8–11$)]. *G*) The luteinizing hormone/testosterone ratio was unaltered when *Cisd2* was disrupted in either LCs or SCs [LC-WT *vs.* LC-KO, $P = 0.6385$; SC-WT *vs.* SC-KO, $P = 0.5115$ (unpaired Stuedent's *t* test; $n = 8–11$)]. Error bars = SEM.

testosterone, damage to steroidogenic machinery as a result of perturbation in the balance between the generation of reactive oxygen species (ROS), and their neutralization by antioxidants, is hypothesized to underlie the decreased testosterone production by aged LCs (21, 23, 24, 94, 96). In other rodent models of premature aging, including the senescence accelerated SAMP8 mouse line (97–99) and premature aging induced by D-galactose administration (100, 101), primary testicular dysfunction is associated with increased testicular ROS production. Studies by Wiley *et al.* (30) demonstrated that CISD2-loss results in a pro-oxidative intracellular environment, which may explain the reduction in testosterone observed in CISD2-KO mice. However, in prematurely aging mitochondrial DNA mutator mice, despite a 7-fold increase in LC superoxide production, testosterone biosynthesis was unaffected; therefore, increased ROS may not be directly toxic to LCs (95). As such, maintenance of LC function in our LC-KO mice

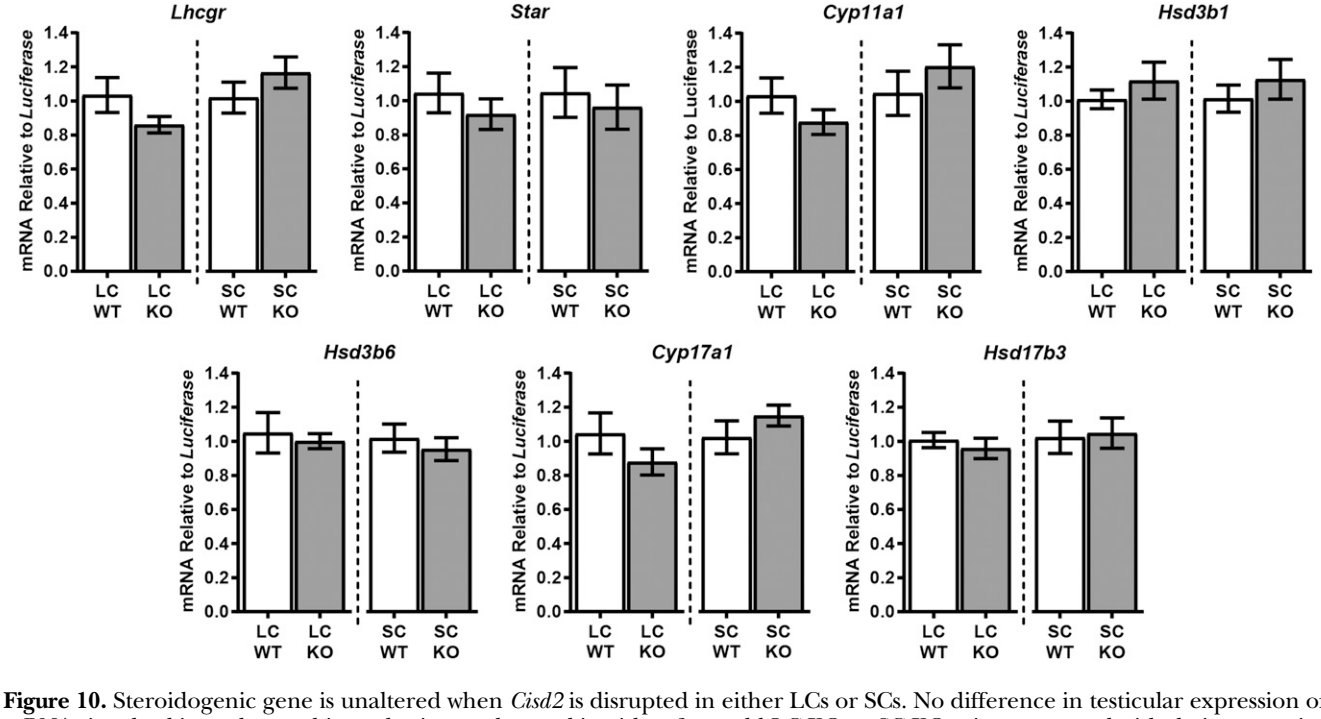

Figure 10. Steroidogenic gene is unaltered when *Cisd2* is disrupted in either LCs or SCs. No difference in testicular expression of mRNAs involved in androgen biosynthesis was observed in either 6-mo-old LC-KO or SC-KO mice compared with their respective WT controls. Luteinizing hormone/chorionic gonadotropin receptor (*Lhcgr*), LC-WT *vs.* LC-KO, $P = 0.1450$; SC-WT *vs.* SC-KO, $P = 0.2838$; steroidogenic acute regulatory protein (*Star*), LC-WT *vs.* LC-KO, $P = 0.4109$; SC-WT *vs.* SC-KO, $P = 6698$; P450 cholesterol side-chain cleavage enzyme (*Cyp11a1*), LC-WT *vs.* LC-KO, (NS) $P = 0.2404$; SC-WT *vs.* SC-KO, $P = 0.4037$; hydroxysteroid dehydrogenase 3-β type 1 (*Hsd3b1*), LC-WT *vs.* LC-KO, $P = 0.3852$; SC-WT *vs.* SC-KO, $P = 0.4390$; hydroxysteroid dehydrogenase 3-β type 6 (*Hsd3b6*), LC-WT *vs.* LC-KO, (NS) $P = 0.7086$; SC-WT *vs.* SC-KO $P = 0.5602$; 17α-hydroxylase, 17,20-lyase (*Cyp17a1*), LC-WT *vs.* LC-KO, $P = 0.2627$; SC-WT *vs.* SC-KO, $P = 0.2924$; hydroxysteroid dehydrogenase 17-β type 3 (*Hsd17b3*), LC-WT *vs.* LC-KO, (NS) $P = 0.5221$; SC-WT *vs.* SC-KO, $P = 0.8524$; $n = 6$–8. Error bars = SEM.

supports the hypothesis of Chen *et al.* (26), stating that alterations in factors extrinsic to LCs may be responsible for impaired steroidogenic function of the aged testis. This would also be in agreement with the reported rejuvenation of aging tissues by exposure to a young systemic milieu in models of heterochronic parabiosis (102–106) and, with the observation that activity of aged stem cells is restored after transplantation into young hosts (107).

Drawing comparisons between prematurely aging, constitutive CISD2-KO mice and our conditional LC-KO and SC-KO models effectively enables the separation of cell intrinsic aging and systemic aging effects on LC function. In the present studies, we noted that circulating corticosterone was significantly elevated in constitutive CISD2-KO mice but not in LC- or SC-conditional KO mice. Because glucocorticoids are known to suppress testicular androgen biosynthesis (63–69), this may offer a partial explanation as to why LC function is impaired in constitutive-KO, but not in LC-KO or SC-KO, animals. The balance of intercellular, bioactive glucocorticoid is regulated by HSD11B enzymes, which are responsible for interconversion between active (corticosterone) and inactive (11-dehydrocorticosterone) forms. Although we did not assess enzymatic activity specifically within LCs we did note a difference in testicular expression of *Hsd11b2*, but not *Hsd11b1*, in constitutive-KO mice. This may represent an inadequate response to elevated corticosterone, leaving LCs in constitutive-KO mice unprotected from the suppressive effects of glucocorticoid on steroidogenesis.

Although old animals may be considered the simplest rodent models of aging, significant time, cost, and welfare implications, concomitant with the generation of naturally aged animals, limit their practicality. Furthermore, aging represents a multifactorial series of complex changes across multiple systems, making it difficult to assign cell/tissue specific contributions to age-related dysfunction. Although mouse models of accelerated aging may not fully model the natural aging process, they have been employed as alternatives to shed light on the mechanisms underpinning degenerative processes associated with aging (27). The testicular phenotype in constitutive CISD2-KO mice closely resembles that of the aging human testis, rendering this line a useful tool for the expedited study of testicular aging. Furthermore, in contrast to naturally aged mice, the hormonal profile of CISD2-KO animals may better reflect the status of the HPG axis in aging men, thus providing a useful resource to test novel therapeutic interventions aimed at reversing age-related primary hypogonadism. Based on our observations of both LC and SC conditional *Cisd2*-KO models, we suggest that, in addition to intrinsic LC aging, age-related disruption to the testicular microenvironment and/or wider endocrine milieu, likely has a significant role in age-associated LC dysfunction. FJ

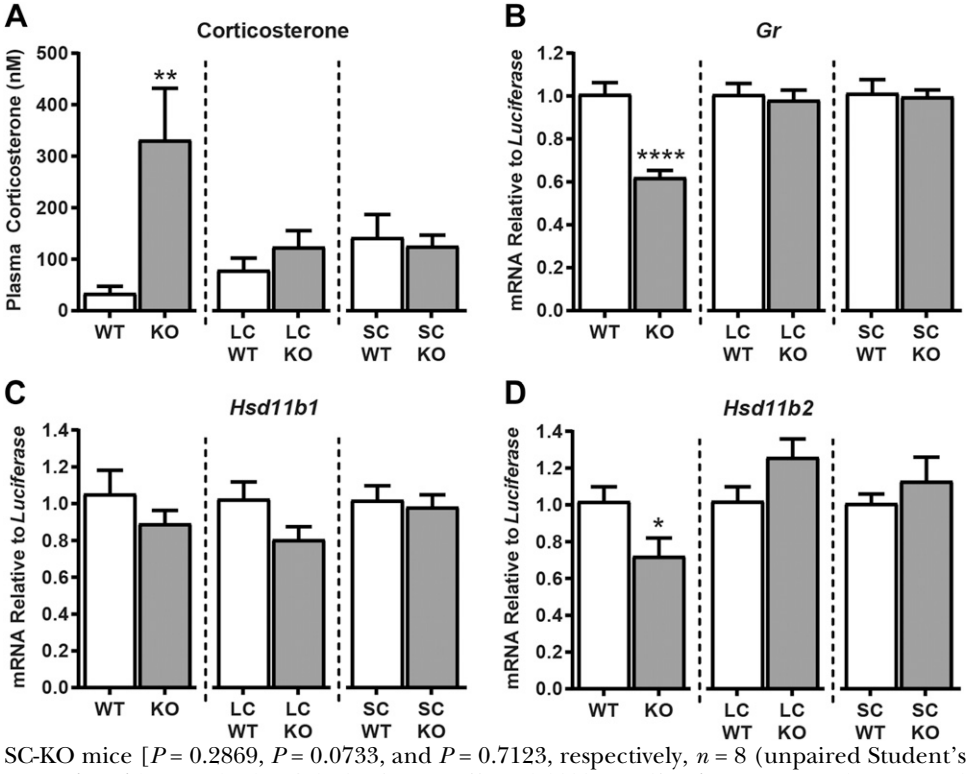

Figure 11. Increased circulating corticosterone in CISD2-deficient mice. *A*) Circulating corticosterone was increased in constitutive CISD2-KO mice at ~6 mo of age. $^{**}P = 0.0054$ (unpaired Student's *t* test; $n = 12$), but not in 6-mo-old LC-KO or SC-KO mice [LC-WT *vs.* LC-KO, $P = 0.2806$; $n = 8$; SC-WT *vs.* SC-KO, (NS) $P = 0.6807$; $n = 10–11$ (unpaired Student's *t* test)]. *B*) Testicular mRNA expression of the glucocorticoid receptor was decreased in constitutive CISD2-KO mice (*Gr*). $^{****}P < 0.0001$ (unpaired Student's *t* test; $n = 8$), whereas expression was normal in LC-KO and SC-KO mice compared with their respective controls [LC-WT *vs.* LC-KO, (NS) $P = 0.7052$; $n = 8$; SC-WT *vs.* SC-KO, (NS) $P = 0.8109$; $n = 8$ (unpaired Student's *t* test)]. *C*) Testicular mRNA expression of *Hsd11b1* was normal in constitutive CISD2-KO, LC-KO, and SC-KO mice [$P = 0.2869$, $P = 0.0733$, and $P = 0.7123$, respectively, $n = 8$ (unpaired Student's *t* test)]. *D*) Expression of *Hsd11b2* was reduced in constitutive CISD2-KO testes ($^{*}P = 0.0322$; $n = 8$), whereas expression was maintained both in LC-KO and SC-KO testes [$P = 0.0806$ and $P = 0.4049$, respectively (unpaired Student's *t* test; $n = 8$)].

ACKNOWLEDGMENTS

The authors thank Nathan Jeffery and Mike Dodds [both from the Medical Research Council (MRC) Centre for Reproductive Health] for technical support. This work was supported by a Biotechnology and Biological Sciences Research Council Doctoral Training Partnerships (BBSRC DTP) Grant BB/J01446X/1 and a Medical Research Council Programme Grant MR/N002970/1 (to L.B.S.) and by the International Center for Research and Research Training in Endocrine Disrupting Effects of Male Reproduction and Child Health (EDMaRC). The authors declare no conflicts of interest.

AUTHOR CONTRIBUTIONS

M. Curley and L. B. Smith designed the study; M. Curley, L. Milne, S. Smith, A. Jørgensen, and H. Frederiksen performed the experimental work; M. Curley, P. Hadoke, and L. B. Smith analyzed the results; P. Potter provided research tools; and M. Curley and L. B. Smith wrote the manuscript.

REFERENCES

1. Perheentupa, A., and Huhtaniemi, I. (2009) Aging of the human ovary and testis. *Mol. Cell. Endocrinol.* **299**, 2–13
2. Gunes, S., Hekim, G. N. T., Arslan, M. A., and Asci, R. (2016) Effects of aging on the male reproductive system. *J. Assist. Reprod. Genet.* **33**, 441–454
3. Morley, J. E., Kaiser, F. E., Perry, H. M. III, Patrick, P., Morley, P. M. K., Stauber, P. M., Vellas, B., Baumgartner, R. N., and Garry, P. J. (1997) Longitudinal changes in testosterone, luteinizing hormone, and follicle-stimulating hormone in healthy older men. *Metabolism* **46**, 410–413
4. Harman, S. M., Metter, E. J., Tobin, J. D., Pearson, J., and Blackman, M. R.; Baltimore Longitudinal Study of Aging. (2001) Longitudinal effects of aging on serum total and free testosterone levels in healthy men. *J. Clin. Endocrinol. Metab.* **86**, 724–731
5. Feldman, H. A., Longcope, C., Derby, C. A., Johannes, C. B., Araujo, A. B., Coviello, A. D., Bremner, W. J., and McKinlay, J. B. (2002) Age trends in the level of serum testosterone and other hormones in middle-aged men: longitudinal results from the Massachusetts male aging study. *J. Clin. Endocrinol. Metab.* **87**, 589–598
6. Wu, F. C., Tajar, A., Pye, S. R., Silman, A. J., Finn, J. D., O'Neill, T. W., Bartfai, G., Casanueva, F., Forti, G., Giwercman, A., Huhtaniemi, I. T., Kula, K., Punab, M., Boonen, S., and Vanderschueren, D.; European Male Aging Study Group. (2008) Hypothalamic-pituitary–testicular axis disruptions in older men are differentially linked to age and modifiable risk factors: the European Male Aging Study. *J. Clin. Endocrinol. Metab.* **93**, 2737–2745
7. Fabbri, E., An, Y., Gonzalez-Freire, M., Zoli, M., Maggio, M., Studenski, S. A., Egan, J. M., Chia, C. W., and Ferrucci, L. (2016) Bioavailable testosterone linearly declines over a wide age spectrum in men and women from the Baltimore Longitudinal Study of Aging. *J. Gerontol. A Biol. Sci. Med. Sci.* **71**, 1202–1209
8. Brand, J. S., Rovers, M. M., Yeap, B. B., Schneider, H. J., Tuomainen, T. P., Haring, R., Corona, G., Onat, A., Maggio, M., Bouchard, C., Tong, P. C., Chen, R. Y., Akishita, M., Gietema, J. A., Gannagé-Yared, M. H., Undén, A. L., Hautanen, A., Goncharov, N. P., Kumanov, P., Chubb, S. A., Almeida, O. P., Wittchen, H. U., Klotsche, J., Wallaschofski, H., Völzke, H., Kauhanen, J., Salonen, J. T., Ferrucci, L., and van der Schouw, Y. T. (2014) Testosterone, sex hormone-binding globulin and the metabolic syndrome in men: an individual participant data meta-analysis of observational studies. *PLoS One* **9**, e100409
9. Pye, S. R., Huhtaniemi, I. T., Finn, J. D., Lee, D. M., O'Neill, T. W., Tajar, A., Bartfai, G., Boonen, S., Casanueva, F. F., Forti, G., Giwercman, A., Han, T. S., Kula, K., Lean, M. E., Pendleton, N., Punab, M., Rutter, M. K., Vanderschueren, D., and Wu, F. C.; EMAS Study Group. (2014) Late-onset hypogonadism and mortality in aging men. *J. Clin. Endocrinol. Metab.* **99**, 1357–1366
10. Farrell, J. B., Deshmukh, A., and Baghaie, A. A. (2008) Low testosterone and the association with type 2 diabetes. *Diabetes Educ.* **34**, 799–806
11. Kupelian, V., Page, S. T., Araujo, A. B., Travison, T. G., Bremner, W. J., and McKinlay, J. B. (2006) Low sex hormone-binding globulin,

total testosterone, and symptomatic androgen deficiency are associated with development of the metabolic syndrome in nonobese men. *J. Clin. Endocrinol. Metab.* **91**, 843–850
12. Kupelian, V., Hayes, F. J., Link, C. L., Rosen, R., and McKinlay, J. B. (2008) Inverse association of testosterone and the metabolic syndrome in men is consistent across race and ethnic groups. *J. Clin. Endocrinol. Metab.* **93**, 3403–3410
13. Yeap, B. B., Knuiman, M. W., Divitini, M. L., Handelsman, D. J., Beilby, J. P., Beilin, J., McQuillan, B., and Hung, J. (2014) Differential associations of testosterone, dihydrotestosterone and oestradiol with physical, metabolic and health-related factors in community-dwelling men aged 17-97 years from the Busselton Health Survey. *Clin. Endocrinol. (Oxf.)* **81**, 100–108
14. Yeap, B. B., Manning, L., Chubb, S. A. P., Handelsman, D. J., Almeida, O. P., Hankey, G. J., and Flicker, L. (2018) Progressive impairment of testicular endocrine function in ageing men: testosterone and dihydrotestosterone decrease, and luteinizing hormone increases, in men transitioning from the 8th to 9th decades of life. *Clin. Endocrinol. (Oxf.)* **88**, 88–95
15. Chen, H., Hardy, M. P., and Zirkin, B. R. (2002) Age-related decreases in Leydig cell testosterone production are not restored by exposure to LH in vitro. *Endocrinology* **143**, 1637–1642
16. Chen, H., Liu, J., Luo, L., and Zirkin, B. R. (2004) Dibutyryl cyclic adenosine monophosphate restores the ability of aged Leydig cells to produce testosterone at the high levels characteristic of young cells. *Endocrinology* **145**, 4441–4446
17. Luo, L., Chen, H., and Zirkin, B. R. (1996) Are Leydig cell steroidogenic enzymes differentially regulated with aging? *J. Androl.* **17**, 509–515
18. Luo, L., Chen, H., and Zirkin, B. R. (2001) Leydig cell aging: steroidogenic acute regulatory protein (StAR) and cholesterol side-chain cleavage enzyme. *J. Androl.* **22**, 149–156
19. Culty, M., Luo, L., Yao, Z. X., Chen, H., Papadopoulos, V., and Zirkin, B. R. (2002) Cholesterol transport, peripheral benzodiazepine receptor, and steroidogenesis in aging Leydig cells. *J. Androl.* **23**, 439–447
20. Luo, L., Chen, H., and Zirkin, B. R. (2005) Temporal relationships among testosterone production, steroidogenic acute regulatory protein (StAR), and P450 side-chain cleavage enzyme (P450scc) during Leydig cell aging. *J. Androl.* **26**, 25–31
21. Chen, H., Cangello, D., Benson, S., Folmer, J., Zhu, H., Trush, M. A., and Zirkin, B. R. (2001) Age-related increase in mitochondrial superoxide generation in the testosterone-producing cells of brown Norway rat testes: relationship to reduced steroidogenic function? *Exp. Gerontol.* **36**, 1361–1373
22. Cao, L., Leers-Sucheta, S., and Azhar, S. (2004) Aging alters the functional expression of enzymatic and non-enzymatic anti-oxidant defense systems in testicular rat Leydig cells. *J. Steroid Biochem. Mol. Biol.* **88**, 61–67
23. Luo, L., Chen, H., Trush, M. A., Show, M. D., Anway, M. D., and Zirkin, B. R. (2006) Aging and the brown Norway rat leydig cell antioxidant defense system. *J. Androl.* **27**, 240–247
24. Beattie, M. C., Chen, H., Fan, J., Papadopoulos, V., Miller, P., and Zirkin, B. R. (2013) Aging and luteinizing hormone effects on reactive oxygen species production and DNA damage in rat Leydig cells. *Biol. Reprod.* **88**, 100
25. Chen, H., Huhtaniemi, I., and Zirkin, B. R. (1996) Depletion and repopulation of Leydig cells in the testes of aging brown Norway rats. *Endocrinology* **137**, 3447–3452
26. Chen, H., Guo, J., Ge, R., Lian, Q., Papadopoulos, V., and Zirkin, B. R. (2015) Steroidogenic fate of the Leydig cells that repopulate the testes of young and aged Brown Norway rats after elimination of the preexisting Leydig cells. *Exp. Gerontol.* **72**, 8–15
27. Kõks, S., Dogan, S., Tuna, B. G., González-Navarro, H., Potter, P., and Vandenbroucke, R. E. (2016) Mouse models of ageing and their relevance to disease. *Mech. Ageing Dev.* **160**, 41–53
28. Carrero, D., Soria-Valles, C., and López-Otín, C. (2016) Hallmarks of progeroid syndromes: lessons from mice and reprogrammed cells. *Dis. Model. Mech.* **9**, 719–735
29. Chen, Y. F., Kao, C. H., Chen, Y. T., Wang, C. H., Wu, C. Y., Tsai, C. Y., Liu, F. C., Yang, C. W., Wei, Y. H., Hsu, M. T., Tsai, S. F., and Tsai, T. F. (2009) Cisd2 deficiency drives premature aging and causes mitochondria-mediated defects in mice. *Genes Dev.* **23**, 1183–1194
30. Wiley, S. E., Andreyev, A. Y., Divakaruni, A. S., Karisch, R., Perkins, G., Wall, E. A., van der Geer, P., Chen, Y. F., Tsai, T. F., Simon, M. I., Neel, B. G., Dixon, J. E., and Murphy, A. N. (2013) Wolfram syndrome protein, Miner1, regulates sulphydryl redox status, the unfolded protein response, and Ca^{2+} homeostasis. *EMBO Mol. Med.* **5**, 904–918
31. Wu, C. Y., Chen, Y. F., Wang, C. H., Kao, C. H., Zhuang, H. W., Chen, C. C., Chen, L. K., Kirby, R., Wei, Y. H., Tsai, S. F., and Tsai, T. F. (2012) A persistent level of Cisd2 extends healthy lifespan and delays aging in mice. *Hum. Mol. Genet.* **21**, 3956–3968
32. Foo, S. S., Turner, C. J., Adams, S., Compagni, A., Aubyn, D., Kogata, N., Lindblom, P., Shani, M., Zicha, D., and Adams, R. H. (2006) Ephrin-B2 controls cell motility and adhesion during blood-vessel-wall assembly. *Cell* **124**, 161–173
33. Lécureuil, C., Fontaine, I., Crepieux, P., and Guillou, F. (2002) Sertoli and granulosa cell-specific Cre recombinase activity in transgenic mice. *Genesis* **33**, 114–118
34. Søeborg, T., Frederiksen, H., Johannsen, T. H., Andersson, A.-M., and Juul, A. (2017) Isotope-dilution TurboFlow-LC-MS/MS method for simultaneous quantification of ten steroid metabolites in serum. *Clin. Chim. Acta* **468**, 180–186
35. Rebourcet, D., O'Shaughnessy, P. J., Monteiro, A., Milne, L., Cruickshanks, L., Jeffrey, N., Guillou, F., Freeman, T. C., Mitchell, R. T., and Smith, L. B. (2014) Sertoli cells maintain Leydig cell number and peritubular myoid cell activity in the adult mouse testis. *PLoS One* **9**, e105687
36. O'Hara, L., York, J. P., Zhang, P., and Smith, L. B. (2014) Targeting of GFP-Cre to the mouse Cyp11a1 locus both drives cre recombinase expression in steroidogenic cells and permits generation of Cyp11a1 knock out mice. *PLoS One* **9**, e84541
37. Hutchison, G. R., Scott, H. M., Walker, M., McKinnell, C., Ferrara, D., Mahood, I. K., and Sharpe, R. M. (2008) Sertoli cell development and function in an animal model of testicular dysgenesis syndrome. *Biol. Reprod.* **78**, 352–360
38. O'Hara, L., Welsh, M., Saunders, P. T., and Smith, L. B. (2011) Androgen receptor expression in the caput epididymal epithelium is essential for development of the initial segment and epididymal spermatozoa transit. *Endocrinology* **152**, 718–729
39. Smith, L. B., Milne, L., Nelson, N., Eddie, S., Brown, P., Atanassova, N., O'Bryan, M. K., O'Donnell, L., Rhodes, D., Wells, S., Napper, D., Nolan, P., Lalanne, Z., Cheeseman, M., and Peters, J. (2012) KATNAL1 regulation of sertoli cell microtubule dynamics is essential for spermiogenesis and male fertility. *PLoS Genet.* **8**, e1002697
40. Wang, C. H., Chen, Y. F., Wu, C. Y., Wu, P. C., Huang, Y. L., Kao, C. H., Lin, C. H., Kao, L. S., Tsai, T. F., and Wei, Y. H. (2014) Cisd2 modulates the differentiation and functioning of adipocytes by regulating intracellular Ca^{2+} homeostasis. *Hum. Mol. Genet.* **23**, 4770–4785
41. Rebourcet, D., O'Shaughnessy, P. J., Pitetti, J.-L., Monteiro, A., O'Hara, L., Milne, L., Tsai, Y. T., Cruickshanks, L., Riethmacher, D., Guillou, F., Mitchell, R. T., van't Hof, R., Freeman, T. C., Nef, S., and Smith, L. B. (2014) Sertoli cells control peritubular myoid cell fate and support adult Leydig cell development in the prepubertal testis. *Development* **141**, 2139–2149
42. Jiang, H., Zhu, W.-J., Li, J., Chen, Q.-J., Liang, W.-B., and Gu, Y.-Q. (2014) Quantitative histological analysis and ultrastructure of the aging human testis. *Int. Urol. Nephrol.* **46**, 879–885
43. Morales, E., Horn, R., Pastor, L. M., Santamaría, L., Pallarés, J., Zuasti, A., Ferrer, C., and Canteras, M. (2004) Involution of seminiferous tubules in aged hamsters: an ultrastructural, immunohistochemical and quantitative morphological study. *Histol. Histopathol.* **19**, 445–455
44. Levy, S., Serre, V., Hermo, L., and Robaire, B. (1999) The effects of aging on the seminiferous epithelium and the blood–testis barrier of the Brown Norway rat. *J. Androl.* **20**, 356–365
45. Wright, W. W., Fiore, C., and Zirkin, B. R. (1993) The effect of aging on the seminiferous epithelium of the brown Norway rat. *J. Androl.* **14**, 110–117
46. Paniagua, R., Nistal, M., Amat, P., Rodriguez, M. C., and Martin, A. (1987) Seminiferous tubule involution in elderly men. *Biol. Reprod.* **36**, 939–947
47. Johnson, L., Petty, C. S., and Neaves, W. B. (1986) Age-related variation in seminiferous tubules in men: a stereologic evaluation. *J. Androl.* **7**, 316–322
48. Gosden, R. G., Richardson, D. W., Brown, N., and Davidson, D. W. (1982) Structure and gametogenic potential of seminiferous tubules in ageing mice. *J. Reprod. Fertil.* **64**, 127–133
49. Paniagua, R., Nistal, M., Sáez, F. J., and Fraile, B. (1991) Ultrastructure of the aging human testis. *J. Electron Microsc. Tech.* **19**, 241–260

50. Johnson, L., Grumbles, J. S., Bagheri, A., and Petty, C. S. (1990) Increased germ cell degeneration during postprophase of meiosis is related to increased serum follicle-stimulating hormone concentrations and reduced daily sperm production in aged men. *Biol. Reprod.* **42**, 281–287
51. Rebourcet, D., Darbey, A., Monteiro, A., Soffientini, U., Tsai, Y. T., Handel, I., Pitetti, J.-L., Nef, S., Smith, L. B., and O'Shaughnessy, P. J. (2017) Sertoli cell number defines and predicts germ and Leydig cell population sizes in the adult mouse testis. *Endocrinology* **158**, 2955–2969
52. Chen, H., Ge, R. S., and Zirkin, B. R. (2009) Leydig cells: from stem cells to aging. *Mol. Cell. Endocrinol.* **306**, 9–16
53. Mendis-Handagama, S. M., and Ariyaratne, H. B. (2001) Differentiation of the adult Leydig cell population in the postnatal testis. *Biol. Reprod.* **65**, 660–671
54. Siril Ariyaratne, H. B., Chamindrani Mendis-Handagama, S., Buchanan Hales, D., and Ian Mason, J. (2000) Studies on the onset of Leydig precursor cell differentiation in the prepubertal rat testis. *Biol. Reprod.* **63**, 165–171
55. O'Shaughnessy, P. J., Willerton, L., and Baker, P. J. (2002) Changes in Leydig cell gene expression during development in the mouse. *Biol. Reprod.* **66**, 966–975
56. Davidoff, M. S., Middendorff, R., Enikolopov, G., Riethmacher, D., Holstein, A. F., and Müller, D. (2004) Progenitor cells of the testosterone-producing Leydig cells revealed. *J. Cell Biol.* **167**, 935–944
57. Ge, R. S., Dong, Q., Sottas, C. M., Chen, H., Zirkin, B. R., and Hardy, M. P. (2005) Gene expression in rat leydig cells during development from the progenitor to adult stage: a cluster analysis. *Biol. Reprod.* **72**, 1405–1415
58. Ge, R. S., Dong, Q., Sottas, C. M., Papadopoulos, V., Zirkin, B. R., and Hardy, M. P. (2006) In search of rat stem Leydig cells: identification, isolation, and lineage-specific development. *Proc. Natl. Acad. Sci. USA* **103**, 2719–2724
59. Kilcoyne, K. R., Smith, L. B., Atanassova, N., Macpherson, S., McKinnell, C., van den Driesche, S., Jobling, M. S., Chambers, T. J. G., De Gendt, K., Verhoeven, G., O'Hara, L., Platts, S., Renato de Franca, L., Lara, N. L. M., Anderson, R. A., and Sharpe, R. M. (2014) Fetal programming of adult Leydig cell function by androgenic effects on stem/progenitor cells. *Proc. Natl. Acad. Sci. USA* **111**, E1924–E1932
60. Sapolsky, R. M., Krey, L. C., and McEwen, B. S. (1983) The adrenocortical stress-response in the aged male rat: impairment of recovery from stress. *Exp. Gerontol.* **18**, 55–64
61. Lo, M. J., Kau, M. M., Cho, W. L., and Wang, P. S. (2000) Aging effects on the secretion of corticosterone in male rats. *J. Investig. Med.* **48**, 335–342
62. Purnell, J. Q., Brandon, D. D., Isabelle, L. M., Loriaux, D. L., and Samuels, M. H. (2004) Association of 24-hour cortisol production rates, cortisol-binding globulin, and plasma-free cortisol levels with body composition, leptin levels, and aging in adult men and women. *J. Clin. Endocrinol. Metab.* **89**, 281–287
63. Schaison, G., Durand, F., and Mowszowicz, I. (1978) Effect of glucocorticoids on plasma testosterone in men. *Acta Endocrinol. (Copenh.)* **89**, 126–131
64. Cumming, D. C., Quigley, M. E., and Yen, S. S. C. (1983) Acute suppression of circulating testosterone levels by cortisol in men. *J. Clin. Endocrinol. Metab.* **57**, 671–673
65. Bambino, T. H., and Hsueh, A. J. (1981) Direct inhibitory effect of glucocorticoids upon testicular luteinizing hormone receptor and steroidogenesis in vivo and in vitro. *Endocrinology* **108**, 2142–2148
66. Badrinarayanan, R., Rengarajan, S., Nithya, P., and Balasubramanian, K. (2006) Corticosterone impairs the mRNA expression and activity of 3β- and 17β-hydroxysteroid dehydrogenases in adult rat Leydig cells. *Biochem. Cell Biol.* **84**, 745–754
67. Martin, L. J., and Tremblay, J. J. (2008) Glucocorticoids antagonize cAMP-induced Star transcription in Leydig cells through the orphan nuclear receptor NR4A1. *J. Mol. Endocrinol.* **41**, 165–175
68. Gao, H. B., Shan, L. X., Monder, C., and Hardy, M. P. (1996) Suppression of endogenous corticosterone levels in vivo increases the steroidogenic capacity of purified rat Leydig cells in vitro. *Endocrinology* **137**, 1714–1718
69. Hales, D. B., and Payne, A. H. (1989) Glucocorticoid-mediated repression of P450scc mRNA and de novo synthesis in cultured Leydig cells. *Endocrinology* **124**, 2099–2104
70. Ramamoorthy, S., and Cidlowski, J. A. (2013) Ligand-induced repression of the glucocorticoid receptor gene is mediated by an NCoR1 repression complex formed by long-range chromatin interactions with intragenic glucocorticoid response elements. *Mol. Cell. Biol.* **33**, 1711–1722
71. Ing, N. H., Forrest, D. W., Riggs, P. K., Loux, S., Love, C. C., Brinsko, S. P., Varner, D. D., and Welsh, T. H., Jr. (2014) Dexamethasone acutely down-regulates genes involved in steroidogenesis in stallion testes. *J. Steroid Biochem. Mol. Biol.* **143**, 451–459
72. Mahmoud, A. M., Goemaere, S., El-Garem, Y., Van Pottelbergh, I., Comhaire, F. H., and Kaufman, J. M. (2003) Testicular volume in relation to hormonal indices of gonadal function in community-dwelling elderly men. *J. Clin. Endocrinol. Metab.* **88**, 179–184
73. Yang, H., Chryssikos, T., Houseni, M., Alzeair, S., Sansovini, M., Iruvuri, S., Torigian, D. A., Zhuang, H., Dadparvar, S., Basu, S., and Alavi, A. (2011) The effects of aging on testicular volume and glucose metabolism: an investigation with ultrasonography and FDG-PET. *Mol. Imaging Biol.* **13**, 391–398
74. Xia, Y., Zhu, W., and Li, J. (2011) Stereological analysis of peritubular cells in aging mouse testes. *J. Reprod. Contraception* **22**, 107–112
75. Vermeulen, A., Kaufman, J. M., Deslypere, J. P., and Thomas, G. (1993) Attenuated luteinizing hormone (LH) pulse amplitude but normal LH pulse frequency, and its relation to plasma androgens in hypogonadism of obese men. *J. Clin. Endocrinol. Metab.* **76**, 1140–1146
76. Tajar, A., Forti, G., O'Neill, T. W., Lee, D. M., Silman, A. J., Finn, J. D., Bartfai, G., Boonen, S., Casanueva, F. F., Giwercman, A., Han, T. S., Kula, K., Labrie, F., Lean, M. E., Pendleton, N., Punab, M., Vanderschueren, D., Huhtaniemi, I. T., and Wu, F. C.; EMAS Group. (2010) Characteristics of secondary, primary, and compensated hypogonadism in aging men: evidence from the European Male Ageing Study. *J. Clin. Endocrinol. Metab.* **95**, 1810–1818
77. Tajar, A., Huhtaniemi, I. T., O'Neill, T. W., Finn, J. D., Pye, S. R., Lee, D. M., Bartfai, G., Boonen, S., Casanueva, F. F. F., Forti, G., Giwercman, A., Han, T. S., Kula, K., Labrie, F., Lean, M. E. J., Pendleton, N., Punab, M., Vanderschueren, D., and Wu, F. C.; EMAS Group. (2012) Characteristics of androgen deficiency in late-onset hypogonadism: results from the European Male Aging Study (EMAS). *J. Clin. Endocrinol. Metab.* **97**, 1508–1516
78. Bronson, F. H., and Desjardins, C. (1977) Reproductive failure in aged CBF1 male mice: interrelationships between pituitary gonadotropic hormones, testicular function, and mating success. *Endocrinology* **101**, 939–945
79. Coquelin, A., and Desjardins, C. (1982) Luteinizing hormone and testosterone secretion in young and old male mice. *Am. J. Physiol.* **243**, E257–E263
80. Eleftheriou, B. E., and Lucas, L. A. (1974) Age-related changes in testes, seminal vesicles and plasma testosterone levels in male mice. *Gerontologia* **20**, 231–238
81. Finch, C. E., Jonec, V., Wisner, J. R., Jr., Sinha, Y. N., de Vellis, J. S., and Swerdloff, R. S. (1977) Hormone production by the pituitary and testes of male C57BL/6J mice during aging. *Endocrinology* **101**, 1310–1317
82. Nelson, J. F., Latham, K. R., and Finch, C. E. (1975) Plasma testosterone levels in C57BL/6J male mice: effects of age and disease. *Acta Endocrinol. (Copenh.)* **80**, 744–752
83. Chu, Y., Huddleston, G. G., Clancy, A. N., Harris, R. B. S., and Bartness, T. J. (2010) Epididymal fat is necessary for spermatogenesis, but not testosterone production or copulatory behavior. *Endocrinology* **151**, 5669–5679
84. Kaufman, J. M., and Vermeulen, A. (2005) The decline of androgen levels in elderly men and its clinical and therapeutic implications. *Endocr. Rev.* **26**, 833–876
85. Vermeulen, A., and Verdonck, L. (1968) Studies on the binding of testosterone to human plasma. *Steroids* **11**, 609–635
86. Joseph, D. R., O'Brien, D. A., Sullivan, P. M., Becchis, M., Tsuruta, J. K., and Petrusz, P. (1997) Overexpression of androgen-binding protein/sex hormone-binding globulin in male transgenic mice: tissue distribution and phenotypic disorders. *Biol. Reprod.* **56**, 21–32
87. Wang, Y. M., Sullivan, P. M., Petrusz, P., Yarbrough, W., and Joseph, D. R. (1989) The androgen-binding protein gene is expressed in CD1 mouse testis. *Mol. Cell. Endocrinol.* **63**, 85–92
88. Hu, X., Tang, Z., Li, Y., Liu, W., Zhang, S., Wang, B., Tian, Y., Zhao, Y., Ran, H., Liu, W., Feng, G.-S., Shuai, J., Wang, H., and Lu, Z. (2015) Deletion of the tyrosine phosphatase Shp2 in Sertoli cells causes infertility in mice. *Sci. Rep.* **5**, 12982

89. Neaves, W. B., Johnson, L., and Petty, C. S. (1985) Age-related change in numbers of other interstitial cells in testes of adult men: evidence bearing on the fate of Leydig cells lost with increasing age. *Biol. Reprod.* **33**, 259–269
90. Neaves, W. B., Johnson, L., Porter, J. C., Parker, C. R., Jr., and Petty, C. S. (1984) Leydig cell numbers, daily sperm production, and serum gonadotropin levels in aging men. *J. Clin. Endocrinol. Metab.* **59**, 756–763
91. Kaler, L. W., and Neaves, W. B. (1978) Attrition of the human Leydig cell population with advancing age. *Anat. Rec.* **192**, 513–518
92. Petersen, P. M., Seierøe, K., and Pakkenberg, B. (2015) The total number of Leydig and Sertoli cells in the testes of men across various age groups - a stereological study. *J. Anat.* **226**, 175–179
93. Wang, C., Leung, A., and Sinha-Hikim, A. P. (1993) Reproductive aging in the male brown-Norway rat: a model for the human. *Endocrinology* **133**, 2773–2781
94. Chen, H., Hardy, M. P., Huhtaniemi, I., and Zirkin, B. R. (1994) Age-related decreased Leydig cell testosterone production in the brown Norway rat. *J. Androl.* **15**, 551–557
95. Shabalina, I. G., Landreh, L., Edgar, D., Hou, M., Gibanova, N., Atanassova, N., Petrovic, N., Hultenby, K., Söder, O., Nedergaard, J., and Svechnikov, K. (2015) Leydig cell steroidogenesis unexpectedly escapes mitochondrial dysfunction in prematurely aging mice. *FASEB J.* **29**, 3274–3286
96. Diemer, T., Allen, J. A., Hales, K. H., and Hales, D. B. (2003) Reactive oxygen disrupts mitochondria in MA-10 tumor Leydig cells and inhibits steroidogenic acute regulatory (StAR) protein and steroidogenesis. *Endocrinology* **144**, 2882–2891
97. Flood, J. F., Farr, S. A., Kaiser, F. E., La Regina, M., and Morley, J. E. (1995) Age-related decrease of plasma testosterone in SAMP8 mice: replacement improves age-related impairment of learning and memory. *Physiol. Behav.* **57**, 669–673
98. Smith, T. B., De Iuliis, G. N., Lord, T., and Aitken, R. J. (2013) The senescence-accelerated mouse prone 8 as a model for oxidative stress and impaired DNA repair in the male germ line. *Reproduction* **146**, 253–262
99. Wang, J. H., Cheng, X. R., Zhang, X. R., Wang, T. X., Xu, W. J., Li, F., Liu, F., Cheng, J. P., Bo, X. C., Wang, S. Q., Zhou, W. X., and Zhang, Y. X. (2016) Neuroendocrine immunomodulation network dysfunction in SAMP8 mice and PrP-hAβPPswe/PS1ΔE9 mice: potential mechanism underlying cognitive impairment. *Oncotarget* **7**, 22988–23005
100. Ahangarpour, A., Oroojan, A. A., and Heidari, H. (2014) Effects of exendin-4 on male reproductive parameters of d-galactose induced aging mouse model. *World J. Mens Health* **32**, 176–183
101. Liao, C.-H., Chen, B.-H., Chiang, H.-S., Chen, C.-W., Chen, M.-F., Ke, C.-C., Wang, Y.-Y., Lin, W.-N., Wang, C.-C., and Lin, Y.-H. (2016) Optimizing a male reproductive aging mouse model by d-galactose injection. *Int. J. Mol. Sci.* **17**, 98–108
102. Conboy, I. M., Conboy, M. J., Wagers, A. J., Girma, E. R., Weissman, I. L., and Rando, T. A. (2005) Rejuvenation of aged progenitor cells by exposure to a young systemic environment. *Nature* **433**, 760–764
103. Ruckh, J. M., Zhao, J. W., Shadrach, J. L., van Wijngaarden, P., Rao, T. N., Wagers, A. J., and Franklin, R. J. (2012) Rejuvenation of regeneration in the aging central nervous system. *Cell Stem Cell* **10**, 96–103
104. Loffredo, F. S., Steinhauser, M. L., Jay, S. M., Gannon, J., Pancoast, J. R., Yalamanchi, P., Sinha, M., Dall'Osso, C., Khong, D., Shadrach, J. L., Miller, C. M., Singer, B. S., Stewart, A., Psychogios, N., Gerszten, R. E., Hartigan, A. J., Kim, M.-J., Serwold, T., Wagers, A. J., and Lee, R. T. (2013) Growth differentiation factor 11 is a circulating factor that reverses age-related cardiac hypertrophy. *Cell* **153**, 828–839
105. Sinha, I., Sinha-Hikim, A. P., Wagers, A. J., and Sinha-Hikim, I. (2014) Testosterone is essential for skeletal muscle growth in aged mice in a heterochronic parabiosis model. *Cell Tissue Res.* **357**, 815–821
106. Katsimpardi, L., Litterman, N. K., Schein, P. A., Miller, C. M., Loffredo, F. S., Wojtkiewicz, G. R., Chen, J. W., Lee, R. T., Wagers, A. J., and Rubin, L. L. (2014) Vascular and neurogenic rejuvenation of the aging mouse brain by young systemic factors. *Science* **344**, 630–634
107. Cao, W., Li, L., Kajiura, S., Amoh, Y., Tan, Y., Liu, F., and Hoffman, R. M. (2016) Aging hair follicles rejuvenated by transplantation to a young subcutaneous environment. *Cell Cycle* **15**, 1093–1098

Received for publication March 28, 2018.
Accepted for publication July 16, 2018.